

Article

A dual-pathway architecture for stress to disrupt agency and promote habit

<https://doi.org/10.1038/s41586-024-08580-w>

Received: 3 October 2023

Accepted: 27 December 2024

Published online: 19 February 2025

 Check for updates

Jacqueline R. Giovanniello¹, Natalie Paredes¹, Anna Wiener¹, Kathia Ramírez-Armenta¹, Chukwuebuka Oragwam¹, Hanniel O. Uwadia¹, Abigail L. Yu², Kayla Lim³, Jenna S. Pimenta¹, Gabriela E. Vilchez¹, Gift Nnamdi¹, Alicia Wang¹, Megha Sehgal¹, Fernando MCV Reis¹, Ana C. Sias¹, Alcino J. Silva^{1,4,5}, Avishek Adhikari^{1,4,5}, Melissa Malvaez¹ & Kate M. Wassum^{1,4,5}✉

Chronic stress can change how we learn and, thus, how we make decisions^{1–5}. Here we investigated the neuronal circuit mechanisms that enable this. Using a multifaceted systems neuroscience approach in male and female mice, we reveal a dual-pathway, amygdala–striatal neuronal circuit architecture by which a recent history of chronic stress disrupts the action–outcome learning underlying adaptive agency and promotes the formation of inflexible habits. We found that the projection from the basolateral amygdala to the dorsomedial striatum is activated by rewarding events to support the action–outcome learning needed for flexible, goal-directed decision-making. Chronic stress attenuates this to disrupt action–outcome learning and, therefore, agency. Conversely, the projection from the central amygdala to the dorsomedial striatum mediates habit formation. Following stress, this pathway is progressively recruited to learning to promote the premature formation of inflexible habits. Thus, stress exerts opposing effects on two amygdala–striatal pathways to disrupt agency and promote habit. These data provide neuronal circuit insights into how chronic stress shapes learning and decision-making, and help understanding of how stress can lead to the disrupted decision-making and pathological habits that characterize substance use disorders and mental health conditions.

When making a decision, we can use what we have learned about our actions and their outcomes to prospectively evaluate the consequences of our potential choices⁶. This goal-directed strategy supports our agency. It allows us to choose actions that cause desirable consequences and avoid those that lead to outcomes that are not beneficial at present. This strategy is, thus, highly flexible. Yet we do not always think about the consequences of our behaviour. Often, this is fine; such habits allow us to efficiently execute routine behaviours on the basis of past success, without forethought of their consequences^{6,7}. The brain balances goal-directed and habitual control to allow behaviour to be adaptive when needed, but efficient when appropriate⁸. Disrupted agency and overreliance on habit can cause inadequate consideration of consequences, disrupted decision-making, inflexible behaviour and a lower threshold for compulsion^{9–11}. This can contribute to cognitive symptoms in numerous diseases, including substance use disorder^{12–14}, obsessive–compulsive disorder¹⁵, obesity¹⁶, schizophrenia^{17,18}, depression^{18,19}, anxiety²⁰ and autism²¹. Chronic stress tips the balance of behavioural control towards habit^{1–5}. Stress can change how we learn and, thus, how we make decisions, by attenuating agency and promoting the formation of inflexible habits. Because stress is a main predisposing factor for addiction and other psychiatric conditions^{22–25}, understanding how stress promotes habit will illuminate an avenue of vulnerability

for these conditions. Yet, despite the importance of understanding adaptive and maladaptive behaviour, little is known of the neuronal circuits that support the learning underlying agency and habits, and even less of those that enable stress to potentiate habit formation.

Amygdala–striatal projections are potential candidate pathways by which stress could influence learning and behavioural control strategy. The dorsomedial striatum (DMS) is an evolutionarily conserved hub for the action–outcome learning that supports goal-directed decision-making^{26,27}. Suppression of DMS activity attenuates such agency and promotes inflexible habits²⁸. The basolateral amygdala (BLA) is also needed for goal-directed behaviour²⁹. It sends a direct excitatory projection to the DMS^{30,31}. Little is known of the function of the BLA→DMS pathway, although it is well-positioned to facilitate the action–outcome learning that supports agency. Conversely, the central amygdala (CeA) has been implicated in habit³². It sends a direct, probably inhibitory³³, projection to the striatum^{30,34,35} and is, thus, poised to oppose striatal activity. Both the BLA and CeA are highly implicated in stress processing^{36,37}. Therefore, we investigated the function of the BLA→DMS and CeA→DMS pathways in action–outcome and habit learning and asked whether chronic stress acts by means of these amygdala–striatal pathways to attenuate agency and promote the formation of inflexible habits.

¹Department of Psychology, University of California, Los Angeles, Los Angeles, CA, USA. ²Department of Physiology, University of California, Los Angeles, Los Angeles, CA, USA. ³Department of Biological Chemistry, University of California, Los Angeles, Los Angeles, CA, USA. ⁴Brain Research Institute, University of California, Los Angeles, Los Angeles, CA, USA. ⁵Integrative Center for Learning and Memory, University of California, Los Angeles, Los Angeles, CA, USA. ✉e-mail: kwassum@ucla.edu

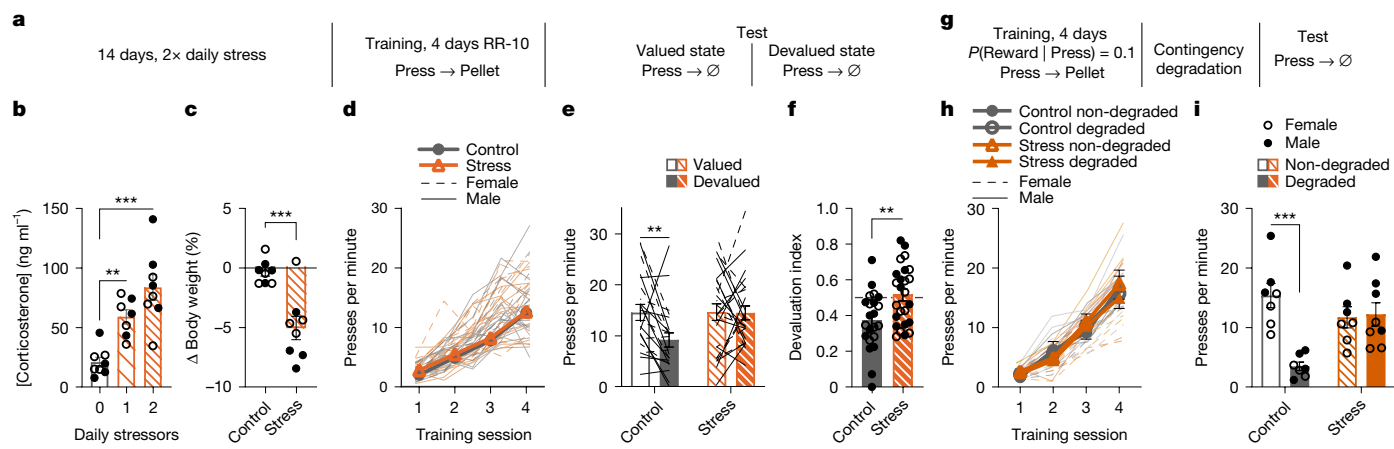


Fig. 1 | Chronic stress disrupts action–outcome learning and potentiates habit formation. **a**, Procedure. Stress, chronic unpredictable mild stress; RR-10, presses earned food pellet rewards on an RR reinforcement schedule before devaluation tests. **b**, Blood serum corticosterone 24 h after 14 days of one stressor per day, two stressors per day, or daily handling (control). One-way ANOVA: Stress $F_{2,20} = 17.35$, $P < 0.0001$. Control, $n = 8$ (4 male); 1x stress, $n = 7$ (3 male); 2x stress, $n = 8$ (4 male). **c**, Per cent change (Δ) in body weight averaged across the first 10 days of stress. Two-sided t -test: $t_{14} = 4.50$, $P = 0.0005$, 95% confidence interval (CI) -6.95 to -2.46 . $n = 8$ mice per group (4 male). **d**, Training press rate (beginning with the last day of FR-1 training). Two-way ANOVA: Training $F_{2,12,95,32} = 168.20$, $P < 0.0001$. Full statistical reporting is given in Supplementary Table 1. **e**, Devaluation test press rate. Two-way ANOVA:

Stress \times Value $F_{1,45} = 4.43$, $P = 0.04$. **f**, Devaluation index ((Devalued condition presses)/(Valued condition presses + Devalued presses)). Two-sided t -test: $t_{45} = 2.99$, $P = 0.005$, 95% CI 0.05 to 0.24. Control, $n = 22$ (13 male); Stress, $n = 25$ (12 male). **g**, Procedure. $P(\text{Reward} \mid \text{Press}) = 0.1$, presses earned pellets with a probability of 0.1 before contingency degradation and test. **h**, Training press rate. Two-way ANOVA: Training $F_{1,66,41,39} = 211.10$, $P < 0.0001$. **i**, Press rate during the post-contingency degradation lever-pressing probe test. Two-way ANOVA: Stress \times Contingency Degradation group $F_{1,25} = 12.75$, $P = 0.002$. Control, non-degraded $n = 7$ (3 male); Control, degraded $n = 7$ (3 male); Stress, non-degraded $n = 7$ (3 male); Stress, degraded $n = 8$ (4 male). Data are presented as mean \pm s.e.m. ** $P < 0.01$, *** $P < 0.001$, corrected for multiple comparisons.

Stress disrupts agency and promotes habit

We first designed a behavioural procedure to model stress-potentiated habit formation in male and female mice (Fig. 1a). Mice received 14 consecutive days of chronic mild unpredictable stress ('stress') including daily, pseudo-random exposure to two of six stressors: damp bedding (4–16 h), tilted cage (4–16 h), white noise (80 dB for 2–16 h), continuous illumination during the dark phase (12 h), physical restraint (2 h) and footshock (0.7 mA, 2–3 s, five shocks per 10 min). This models aspects of the repeated and varied nature of stress experienced by humans, including uncontrollable physical aversive events, disrupted sleep and poor environmental conditions. Controls received equated handling. Demonstrating efficacy, serum corticosterone was higher (Fig. 1b; see Supplementary Table 1 for full statistical reporting) and body weight was lower (Fig. 1c) in stressed mice than in controls. This procedure was intentionally mild to model low-level, chronic stress. Accordingly, it did not cause major anxiety- or depression-like phenotypes in classic assays of such behaviour (Extended Data Fig. 1). At 24 h after the last stressor, mice were trained to lever press to earn a food pellet reward. We used four sessions of training on a random-ratio (RR) schedule of reinforcement in which a variable number of presses (average one to ten, escalated each training session) was required to earn each reward. The tight press–reward relationship of this regime encourages action–outcome learning and, together with the short training duration, the use of such knowledge to support agency and goal-directed decision-making³⁸. Mice were food-deprived and body weight did not differ significantly between control and stressed mice during training (Supplementary Table 2). Both control and stressed mice similarly acquired the instrumental behaviour (Fig. 1d). Thus, stress did not cause general learning, motivational or locomotor impairments. To evaluate the behavioural control strategy, we used a gold standard outcome-specific devaluation test^{6,39}. Mice were given 90 min non-contingent access to the food pellet earned during training to induce a sensory-specific satiety rendering that specific food pellet temporarily devalued. Lever pressing was assessed in a 5 min, non-reinforced probe test immediately following the prefeeding. Performance was compared with that following

satiation on an alternate food pellet to control for general satiety (valued state; test order counterbalanced). Both control and stressed mice consumed similar amounts during the prefeed (Supplementary Table 3), indicating that stress did not alter food consumption. Stress also did not affect food pellet discrimination or devaluation efficacy (Supplementary Table 4). If mice have learned the action–outcome relationship and are using this to support prospective consideration of action consequences for flexible, goal-directed decision-making, they will reduce lever pressing when the outcome is devalued. We saw such agency in control mice (Fig. 1e,f; see also Extended Data Fig. 2 for data on entries into the food delivery port). Stressed mice were insensitive to devaluation, indicating disrupted agency. Such lack of consideration of action consequences marks inflexible habits^{8,26}.

To provide converging evidence that stress disrupts the action–outcome learning that supports agency, we conducted a second experiment, this time assessing behavioural control strategy using the other gold standard test: contingency degradation^{6,40} (Fig. 1g). Mice received chronic stress or daily handling control before being trained to lever press to earn food pellet rewards. During training, each press earned a reward with a probability that became progressively leaner ($P(\text{Reward} \mid \text{Press}) = 1.0$ to 0.1). Control and stressed mice, again, similarly acquired the instrumental behaviour (Fig. 1h). Half the mice in each group received a 20-min contingency degradation session during which lever pressing continued to earn a reward with a probability of 0.1, but a reward was also delivered non-contingently with the same probability ($P(\text{Reward} \mid \text{Press}) = 0.1$, $P(\text{Reward} \mid \text{NoPress}) = 0.1$). Thus, the reward was no longer contingent on pressing. The other half received a non-degraded control session in which rewards remained contingent on pressing ($P(\text{Reward} \mid \text{Press}) = 0.1$, $P(\text{Reward} \mid \text{NoPress}) = 0$) (see Extended Data Fig. 3 for data from the contingency degradation session). Lever pressing was assessed in a 5 min, non-reinforced probe test the next day. If mice learned the action–outcome contingency and used it to support their agency, their actions should be sensitive to the change in this contingent relationship, such that they will reduce lever pressing when it is no longer needed to earn a reward⁴⁰. Controls were sensitive to contingency degradation. Stressed mice were

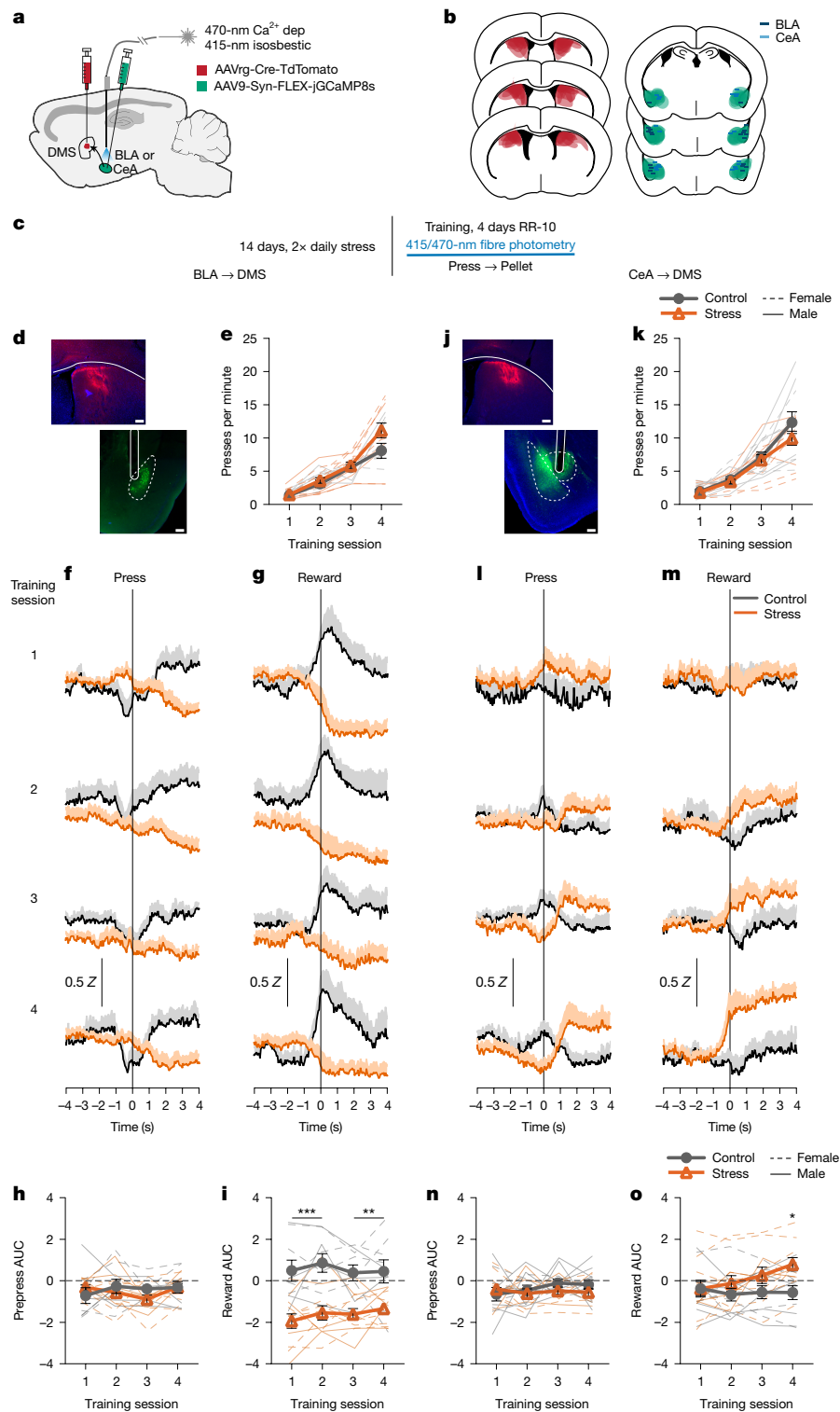


Fig. 2 | Chronic stress attenuates BLA→DMS activity during action-outcome learning and progressively recruits CeA→DMS activity. **a**, Intersectional BLA→DMS or CeA→DMS fibre photometry calcium imaging approach. **b**, Expression and fibre map for all mice. **c**, Procedure. Stress, chronic unpredictable stress; RR-10, random-ratio reinforcement schedule. **d–i**, Fibre photometry recordings of GCaMP8s in BLA→DMS neurons during learning. **d**, Images of retro-Cre expression in DMS and immunofluorescent staining of Cre-dependent GCaMP8s expression and fibre placement in BLA. **e**, Training press rate. Two-way ANOVA: Training $F_{1,72,32,66} = 81.40, P < 0.0001$. **f,g**, Trial-averaged Z-scored $\Delta f/f$ BLA→DMS GCaMP8s fluorescence changes aligned to bout-initiating presses (**f**) and reward collection (**g**) across training. **h,i**, AUC 3 s before initiating presses (**h**) (two-way ANOVA: Training $F_{2,49,47,38} = 0.91, P = 0.43$) or following reward collection (**i**) (two-way ANOVA: Stress $F_{1,19} = 24.13, P < 0.0001$). Control, $n = 9$ (4 male); Stress, $n = 12$ (5 male). **j–o**, Fibre photometry recordings of GCaMP8s in CeA→DMS neurons during learning. **j**, Immunofluorescent image of retro-Cre expression in DMS and Cre-dependent GCaMP8s expression and fibre placement in CeA. **k**, Training press rate. Two-way ANOVA: Training $F_{1,51,30,23} = 65.61, P < 0.0001$. **l,m**, Trial-averaged Z-scored $\Delta f/f$ CeA→DMS GCaMP8s fluorescence changes aligned to bout-initiating presses (**l**) and reward collection (**m**) across training. **n,o**, AUC 3 s before initiating presses (**n**) (two-way ANOVA: Stress $F_{1,20} = 0.74, P = 0.40$) or following reward collection (**o**) (two-way ANOVA: Training × Stress $F_{3,60} = 4.51, P = 0.006$). Control, $n = 11$ (6 male); Stress, $n = 11$ (4 male). Data are presented as mean ± s.e.m.

* $P < 0.05$, ** $P < 0.01$, *** $P < 0.001$, corrected for multiple comparisons. Scale bars, 200 μ m.

not (Fig. 2i). Together these data show that a recent history of chronic stress causes an inability to engage one's agency and flexibly adapt behaviour when its consequence is not beneficial at present or when it is no longer required to earn a reward. Thus, chronic stress disrupts action-outcome learning to attenuate agency and, instead, causes the premature formation of inflexible habits.

Stress oppositely affects BLA→DMS and CeA→DMS

We next confirmed the existence of direct BLA and CeA projections to dorsal striatum using both anterograde and retrograde tracing. We

found that both BLA and CeA directly project to the DMS (Extended Data Fig. 4). We then characterized the activity of these BLA→DMS and CeA→DMS pathways during action-outcome learning and asked whether it is influenced by chronic stress. We used fibre photometry to record fluorescent activity of the genetically encoded calcium indicator GCaMP8s expressed using an intersectional approach in BLA or CeA neurons that project to the DMS (Fig. 2a–j). Mice received chronic stress or daily handling control before being trained to lever press to earn food pellet rewards on a RR reinforcement schedule (Fig. 2c). Both control and stressed mice similarly acquired the instrumental behaviour (Fig. 2e,k, see Extended Data Fig. 5 for food port entry data). Fibre

photometry (473-nm calcium-dependent, 415-nm isosbestic) recordings were made during each training session. BLA→DMS neurons were robustly activated by an earned reward during learning (Fig. 2f–i). Thus, the BLA→DMS pathway is active when mice are able to link the rewarding consequence to their actions, thus forming the action–outcome knowledge that supports agency. This activity was absent in stressed mice (Fig. 2g,i). Chronic stress attenuated the BLA→DMS activity associated with action–outcome learning. Conversely, CeA→DMS neurons were not robustly active during this form of instrumental learning in control mice, indicating that CeA→DMS projection activity is not associated with action–outcome learning. Stress caused the CeA→DMS pathway to be progressively engaged around the earned reward with training (Fig. 2l–o). The CeA→DMS response to an earned reward was long lasting, taking around 30 s to return to baseline after reward collection (Extended Data Fig. 6). Thus, a recent history of chronic stress causes the CeA→DMS pathway to be recruited to instrumental learning. We detected similar patterns in response to unpredicted rewards in both pathways (Extended Data Fig. 6). Both BLA→DMS and CeA→DMS projections were acutely activated by unpredicted aversive events (footshock; Extended Data Fig. 6), indicating that neither BLA→DMS nor CeA→DMS bulk activity is valence-specific. These aversive responses were not altered by stress (Extended Data Fig. 6), providing a positive control for our ability to detect signals in all groups. Chronic stress did, however, reduce post-shock fear-related BLA→DMS activity, consistent with its effects on reward signals in this pathway. Chronic stress did not alter baseline spontaneous calcium activity in either pathway, indicating that it does not generally increase or decrease excitability in these pathways (Extended Data Fig. 6). Together these data indicate that a recent history of chronic stress oppositely modulates BLA→DMS and CeA→DMS pathway activity. BLA→DMS projections are normally activated by rewarding events, but stress prevents this learning-related activity and, instead, causes the CeA→DMS pathway to be progressively recruited during learning.

BLA→DMS mediates agency learning

BLA→DMS projections are activated by rewards to support action–outcome learning for flexible, goal-directed decision-making

BLA→DMS projections are activated by earned rewards. This experience is an opportunity to link the reward to the action that earned it, forming action–outcome knowledge that supports agency. We reasoned that such BLA→DMS activity might be critical for action–outcome learning. If this is true, then inhibiting reward-evoked BLA→DMS activity should suppress action–outcome learning and, thereby, disrupt flexible goal-directed decision-making. We tested this by optogenetically inhibiting BLA→DMS projection activity during instrumental learning. We expressed the inhibitory opsin archaerhodopsin (Arch) or fluorophore control in the BLA and implanted optical fibres in the DMS in the vicinity of Arch-expressing BLA axons and terminals (Fig. 3a,b). Mice were trained to lever press to earn food pellet rewards on an RR reinforcement schedule. We optically (532 nm, 10 mW, 5 s) inhibited BLA terminals in the DMS during each earned reward (Fig. 3c). BLA→DMS inhibition did not affect acquisition of the instrumental behaviour (Fig. 3d; see Extended Data Fig. 7 for food port entry data). Training was followed by a set of outcome-specific devaluation tests, as above. No manipulation was given at test to allow us to isolate BLA→DMS function in action–outcome learning rather than the expression of such learning during decision-making. Controls were sensitive to outcome devaluation, indicating action–outcome learning for goal-directed decision-making. Inhibition of BLA→DMS projections during learning caused subsequent insensitivity to outcome devaluation (Fig. 3e,f). BLA→DMS inhibition was not inherently rewarding or aversive (Extended Data Fig. 8). Thus, BLA→DMS projections are normally activated by rewarding events to enable the action–outcome learning that supports agency.

BLA→DMS activation restores agency after stress

Stress-induced suppression of BLA→DMS activity disrupts action–outcome learning and enables premature habit formation

Because BLA→DMS projections are critical for action–outcome learning, we next reasoned that the stress-induced suppression of BLA→DMS activity might disrupt such learning. We tested this by asking whether activating BLA→DMS projections during learning, to counter the effects of stress, is sufficient to restore action–outcome learning and, thus, goal-directed decision-making in stressed mice. We did this in two ways. Because chronic stress abolishes reward-evoked BLA→DMS activity during learning, we first used optogenetics to stimulate BLA→DMS projections at the time of earned reward during learning following chronic stress. Using an intersectional approach (Fig. 3g), we expressed the excitatory opsin Channelrhodopsin-2 (ChR2) or a fluorophore control in DMS-projecting BLA neurons (Fig. 3h). Following chronic stress or daily handling control, mice were trained to lever press to earn food pellet rewards. We used a random-interval (RI) schedule of reinforcement in which a variable (average 30 s) period had to elapse after an earned reward before a press would earn another reward. Limited training on this regime allows action–outcome learning for goal-directed decision-making⁴¹. However, the looser action–outcome relationship is more permissive for habits than a ratio reinforcement schedule^{38,42}, thereby making it more difficult to neurobiologically prevent stress-potentiated habit and the results more robust were such an effect to occur. We optically (473 nm, 10 mW, 20 Hz, 2 s) stimulated DMS-projecting BLA neurons during collection of each earned reward (Fig. 3i). Neither stress nor BLA→DMS stimulation significantly altered acquisition of the instrumental behaviour (Fig. 3j). Training was followed by the outcome-devaluation test, conducted without manipulation. Whereas controls were sensitive to outcome devaluation, indicating action–outcome learning and flexible goal-directed decision-making, stressed mice were insensitive to devaluation, indicating premature habit formation (Fig. 3l). Optogenetic activation of BLA→DMS projections during learning restored normal action–outcome learning enabling agency, as evidenced by sensitivity to devaluation, in stressed mice (Fig. 3k,l). Thus, activation of BLA→DMS projections during reward learning is sufficient to overcome the effect of previous chronic stress and restore action–outcome learning to enable agency for flexible, goal-directed decision-making.

To provide converging evidence, we conducted a second experiment in which we activated the BLA→DMS pathway during post-stress learning using chemogenetics. Using an intersectional approach (Fig. 3m), we expressed the excitatory designer receptor human M3 muscarinic receptor (hM3Dq) or a fluorophore control in DMS-projecting BLA neurons (Fig. 3n). Following chronic stress or daily handling control, mice were trained to lever press to earn food pellet rewards on an RI schedule of reinforcement (Fig. 3o). Before each instrumental training session, mice received the hM3Dq ligand clozapine N-oxide (CNO; 0.2 mg kg⁻¹ by intraperitoneal injection)^{43,44} to activate BLA→DMS projections. Neither stress nor chemogenetic BLA→DMS activation altered instrumental acquisition (Fig. 3p). Mice then received devaluation tests. Whereas controls were sensitive to outcome devaluation, stressed mice were, again, insensitive to devaluation (Fig. 3q,r). Chemogenetic activation of BLA→DMS projections during learning replicated the effect of optogenetic activation, restoring action–outcome learning to enable goal-directed decision-making, as evidenced by sensitivity to devaluation, in stressed mice (Fig. 3q,r). Neither optogenetic nor chemogenetic activation of BLA→DMS projections significantly affected learning in mice without a history of chronic stress. Behaviour was, however, variable in these groups with some marginal evidence of an influence on action–outcome learning, perhaps due to disruption of neurotypical activity. Together these data show that BLA→DMS projections are activated by rewards to enable the action–outcome learning that supports flexible, goal-directed decision-making and

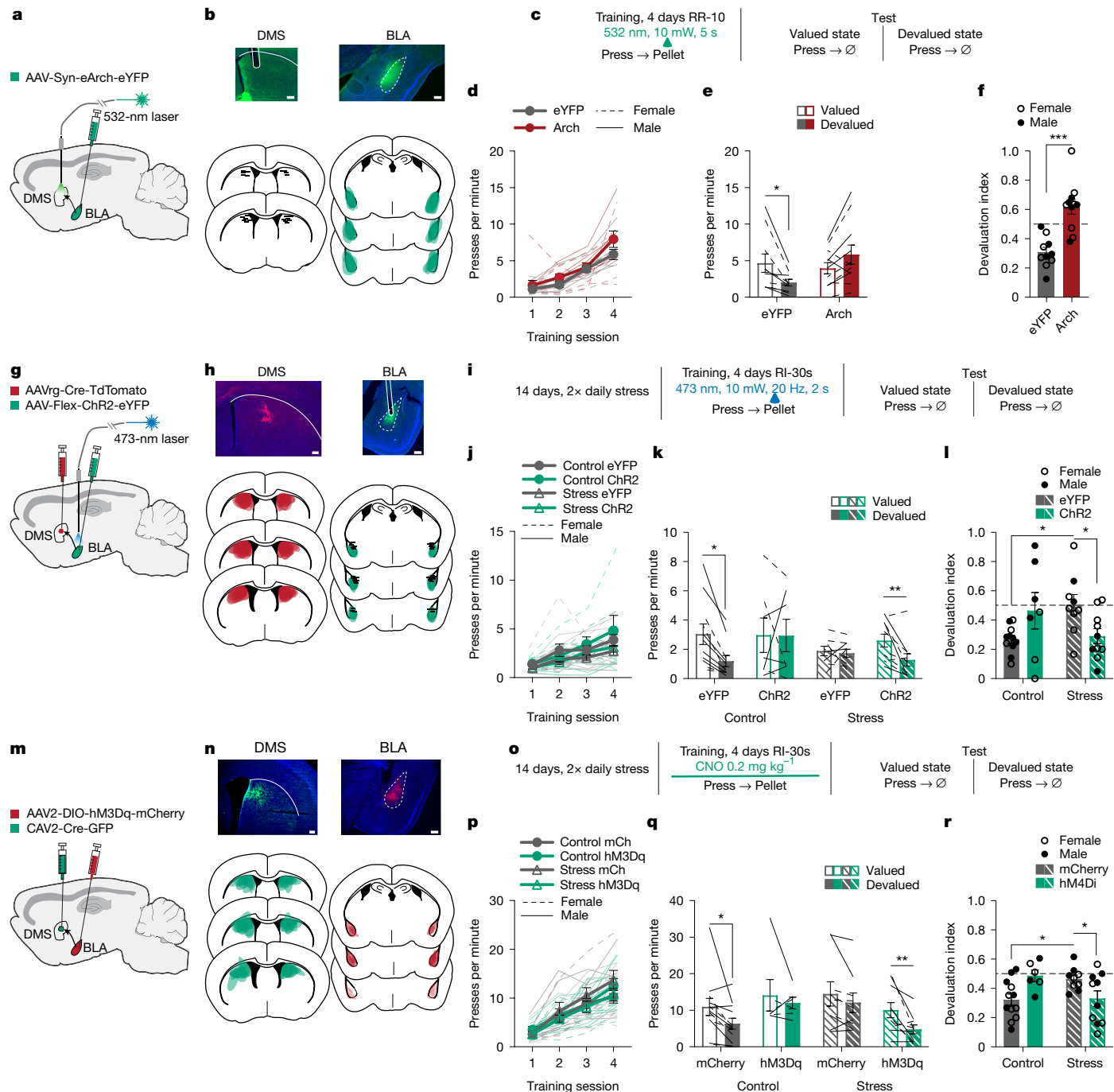


Fig. 3 | BLA→DMS mediates action–outcome learning and is suppressed by stress to disrupt agency and promote habit formation. **a–f**, Optogenetic BLA→DMS inactivation at reward during instrumental learning. **a**, Optogenetic inhibition approach. **b**, Top, immunofluorescent images of Arch expression in BLA and optical fibre tip in the vicinity of Arch-expressing BLA terminals in DMS. Bottom, expression and fibre map for all mice. **c**, Procedure. RR-10, random-ratio reinforcement schedule. **d**, Training press rate. Two-way ANOVA: Training $F_{1.70,32.34} = 41.26, P < 0.0001$. **e**, Devaluation test press rate. Two-way ANOVA: Stress \times Value $F_{1,19} = 14.35, P = 0.001$. **f**, Devaluation index ((Devalued presses)/(Valued presses + Devalued presses)). Two-sided *t*-test: $t_{19} = 5.03, P < 0.0001, 95\% \text{ CI } 0.18 \text{ to } 0.44$. eYFP, $n = 10$ (5 male); Arch, $n = 11$ (5 male). **g–l**, Optogenetic BLA→DMS activation at reward during post-stress learning. **g**, Intersectional optogenetic activation approach. **h**, Top, immunofluorescent images of retro-Cre expression in DMS and Cre-dependent hM3Dq expression in BLA. Bottom, expression map for all mice. **i**, Procedure. Stress, chronic unpredictable stress; RI-30s, random-interval reinforcement schedule. **j**, Training press rate. Two-way ANOVA: Training $F_{1.95,64.18} = 30.17, P < 0.0001$. **k**, Devaluation test press rate. Three-way ANOVA: Value \times Stress \times Virus $F_{1,33} = 6.74, P = 0.01$. Control groups, two-way ANOVA: Value \times Virus $F_{1,16} = 0.3.13, P = 0.10$. Stress groups, two-way ANOVA: Value \times Virus $F_{1,17} = 4.23, P = 0.05$. **l**, Devaluation index. Two-way ANOVA: Stress \times Virus $F_{1,33} = 9.64, P = 0.004$. Control eYFP, $n = 11$ (7 male); Control ChR2, $n = 7$ (4 male); Stress eYFP, $n = 9$ (2 male); Stress ChR2, $n = 10$ (3 male). **m–r**, Chemogenetic BLA→DMS activation during post-stress learning. **m**, Top, immunofluorescent images of retro-Cre expression in DMS and Cre-dependent hM3Dq expression in BLA. Bottom, expression map for all mice. **o**, Procedure. **p**, Training press rate. Two-way ANOVA: Training $F_{2.04,67.36} = 73.32, P < 0.0001$. **q**, Devaluation test press rate. Planned comparisons two-sided *t*-test valued versus devalued: Control mCherry $t_{11} = 2.76, P = 0.01, 95\% \text{ CI } 1.20 \text{ to } 7.97$; Control hM3Dq $t_5 = 0.89, P = 0.38, 95\% \text{ CI } -2.69 \text{ to } 6.89$; Stress mCherry $t_8 = 1.25, P = 0.22, 95\% \text{ CI } -1.51 \text{ to } 6.31$; Stress hM3Dq $t_9 = 2.9, P = 0.007, 95\% \text{ CI } 1.57 \text{ to } 8.99$. **r**, Devaluation index. Two-way ANOVA: Stress \times Virus $F_{1,33} = 11.60, P = 0.002$. Control mCherry, $n = 12$ (7 male); Control hm3Dq, $n = 6$ (3 male); Stress mCherry, $n = 9$ (5 male); Stress hm3Dq, $n = 10$ (5 male). Data presented as mean \pm s.e.m. * $P < 0.05$, ** $P < 0.01$, *** $P < 0.001$, corrected for multiple comparisons. Ø, no reward. Scale bars, 200 μ m.

$P = 0.01$. Control groups, two-way ANOVA: Value \times Virus $F_{1,16} = 0.3.13, P = 0.10$. Stress groups, two-way ANOVA: Value \times Virus $F_{1,17} = 4.23, P = 0.05$. **l**, Devaluation index. Two-way ANOVA: Stress \times Virus $F_{1,33} = 9.64, P = 0.004$. Control eYFP, $n = 11$ (7 male); Control ChR2, $n = 7$ (4 male); Stress eYFP, $n = 9$ (2 male); Stress ChR2, $n = 10$ (3 male). **m–r**, Chemogenetic BLA→DMS activation during post-stress learning. **m**, Top, immunofluorescent images of retro-Cre expression in DMS and Cre-dependent hM3Dq expression in BLA. Bottom, expression map for all mice. **o**, Procedure. **p**, Training press rate. Two-way ANOVA: Training $F_{2.04,67.36} = 73.32, P < 0.0001$. **q**, Devaluation test press rate. Planned comparisons two-sided *t*-test valued versus devalued: Control mCherry $t_{11} = 2.76, P = 0.01, 95\% \text{ CI } 1.20 \text{ to } 7.97$; Control hM3Dq $t_5 = 0.89, P = 0.38, 95\% \text{ CI } -2.69 \text{ to } 6.89$; Stress mCherry $t_8 = 1.25, P = 0.22, 95\% \text{ CI } -1.51 \text{ to } 6.31$; Stress hM3Dq $t_9 = 2.9, P = 0.007, 95\% \text{ CI } 1.57 \text{ to } 8.99$. **r**, Devaluation index. Two-way ANOVA: Stress \times Virus $F_{1,33} = 11.60, P = 0.002$. Control mCherry, $n = 12$ (7 male); Control hm3Dq, $n = 6$ (3 male); Stress mCherry, $n = 9$ (5 male); Stress hm3Dq, $n = 10$ (5 male). Data presented as mean \pm s.e.m. * $P < 0.05$, ** $P < 0.01$, *** $P < 0.001$, corrected for multiple comparisons. Ø, no reward. Scale bars, 200 μ m.

chronic stress attenuates this to disrupt agency and promote premature habit formation.

CeA→DMS mediates habit formation

CeA→DMS projections mediate the formation of routine habits

The CeA is necessary for habit³². This function may be achieved, at least in part, through its direct inhibitory projection to the DMS. It is, therefore, perhaps not surprising that the CeA→DMS pathway is not typically active during action–outcome learning. Rather the CeA is activated by rewards following overtraining⁴⁵. We reasoned that the CeA→DMS pathway might mediate the natural habit formation that occurs for routine behaviours. To test this, we asked whether CeA→DMS projection activity is necessary for habit formation by optogenetically inhibiting CeA→DMS projections at the time of earned reward during learning and overtraining. We expressed the inhibitory opsin Arch or a fluorophore control in the CeA and implanted optical fibres in the DMS in the vicinity of Arch-expressing CeA axons and terminals (Fig. 4a–c). Mice were trained to lever press to earn food pellet rewards on an RI schedule of reinforcement and were overtrained to promote natural habit formation (Fig. 4c). We optically (532 nm, 10 mW, 5 s) inhibited CeA terminals in the DMS during each earned reward (Fig. 4c). Training was followed by the devaluation test. No manipulation was given on test to allow us to isolate CeA→DMS function in habit learning from habit expression. Optogenetic CeA→DMS inhibition did not alter acquisition of the instrumental behaviour (Fig. 4d; see Extended Data Fig. 9 for food port entry data). It did, however, prevent habit formation. Controls formed routine habits, evidenced by insensitivity to devaluation. Mice for which we inhibited the CeA→DMS pathway during overtraining continued to show flexible goal-directed decision-making, sensitivity to devaluation (Fig. 4e,f). Thus, the CeA→DMS pathway mediates the natural habit formation that occurs with repeated practice of an instrumental routine.

Stress promotes habit via CeA→DMS

Stress-induced recruitment of CeA→DMS activity mediates premature habit formation

Given that the CeA→DMS pathway mediates habit formation, we next reasoned that the stress-induced recruitment of this pathway to learning may enable stress to promote premature habit formation. If this is true, then preventing the stress-induced increase in CeA→DMS activity during learning should prevent premature habit formation and restore action–outcome learning and, therefore, agency. We tested this in two ways. Because chronic stress engages the CeA→DMS pathway at reward experience during learning, we first optogenetically inhibited CeA→DMS projections at the time of earned reward during learning following stress. We expressed the inhibitory opsin Arch or a fluorophore control in the CeA and implanted optical fibres in the DMS (Fig. 4g,h). Following chronic stress or daily handling control, mice were trained to lever press to earn food pellet rewards and we optically (532 nm, 10 mW, 5 s) inhibited CeA terminals in the DMS during each earned reward (Fig. 4i). We used an RI schedule of reinforcement to increase the robustness of the results. Neither stress nor CeA→DMS inhibition altered acquisition of the instrumental behaviour (Fig. 4j). Training was followed by devaluation tests, conducted without manipulation. At test, we again found evidence of goal-directed decision-making, sensitivity to devaluation, in control mice and potentiated habit formation, insensitivity to devaluation, in stressed mice (Fig. 4k,l). Optogenetic inhibition of CeA→DMS activity at reward during learning restored action–outcome learning to enable goal-directed decision-making in stressed mice, as evidenced by sensitivity to devaluation (Fig. 4k,l). Thus, stress-induced activation of CeA→DMS projections during reward learning is necessary to promote premature habit formation.

To provide converging evidence, we conducted a second experiment in which we chemogenetically inhibited CeA→DMS projections during learning following stress. We used an intersectional approach (Fig. 4m) to express the inhibitory designer receptor human M4 muscarinic receptor (hM4Di) or a fluorophore control in DMS-projecting CeA neurons (Fig. 4m,n). Following chronic stress or daily handling control, mice were trained to lever press to earn food pellet rewards on an RI reinforcement schedule (Fig. 4o). Before each training session, mice received the hM4Di ligand CNO (2.0 mg kg⁻¹ by intraperitoneal injection)^{46,47} to inactivate CeA→DMS projections. Neither stress nor chemogenetic CeA→DMS inactivation altered acquisition of the instrumental behaviour (Fig. 4p). Chemogenetic inhibition of CeA→DMS projections during learning replicated the effects of optogenetic inhibition, restoring action–outcome learning to enable goal-directed decision-making, sensitivity to devaluation, in stressed mice (Fig. 4q,r). Neither optogenetic nor chemogenetic CeA→DMS inhibition significantly affected learning or behavioural control strategy in mice without a history of chronic stress. Together, these data indicate that chronic stress engages CeA→DMS projections during subsequent reward learning experience to promote the premature formation of inflexible habits.

CeA→DMS projection activity is sufficient to promote premature habit formation following subthreshold chronic stress

We next asked whether CeA→DMS pathway activity at reward during learning is sufficient to promote habit formation. We used an intersectional approach (Fig. 4s) to express the excitatory opsin ChR2 or a fluorophore control in DMS-projecting CeA neurons and implanted optic fibres above the CeA (Fig. 4t). We first optically (473 nm, 10 mW, 20 Hz, 25-ms pulse width, 2 s) stimulated CeA→DMS neurons with each earned reward during instrumental learning on an RR schedule of reinforcement in mice without a history of chronic stress. This affected neither acquisition of the lever-press behaviour nor the action–outcome learning needed to support flexible, goal-directed decision-making during the devaluation test (Extended Data Fig. 10). Thus, activation of the CeA→DMS pathway during reward learning experience alone is not sufficient to disrupt action–outcome learning or promote habit formation.

We next reasoned that activation of CeA→DMS projections might be sufficient to tip the balance of behavioural control towards habit in the context of a very mild chronic stress experience. To test this, we repeated the experiment in mice with a history of once-daily stress for 14 consecutive days (Fig. 4s–u). Again, neither CeA→DMS activation nor stress altered acquisition of the instrumental behaviour (Fig. 4v). Less-frequent chronic stress was itself insufficient to cause premature habit formation. Mice were sensitive to devaluation, indicating preserved action–outcome learning and agency (Fig. 4w,x). Activation of CeA→DMS projections at reward during learning was sufficient to cause premature habit formation, as evidenced by greater insensitivity to devaluation in mice that received stimulation relative to those that did not (Fig. 4w,x). Thus, activation of CeA→DMS projections during learning is sufficient to amplify the effects of previous subthreshold chronic stress to promote habit formation. CeA→DMS stimulation was not inherently rewarding or aversive in either control or stressed mice (Extended Data Fig. 8). Together, these data indicate that chronic stress recruits the CeA→DMS pathway to subsequent learning to promote the premature formation of inflexible habits.

Discussion

These data show a dual-pathway neuronal circuit architecture by which a recent history of chronic stress shapes learning to disrupt adaptive agency and promote inflexible habits. Both the BLA and CeA send direct projections to the DMS. The BLA→DMS pathway is activated by rewarding events to support the action–outcome learning needed for flexible, goal-directed decision-making. Chronic stress attenuates this

Article

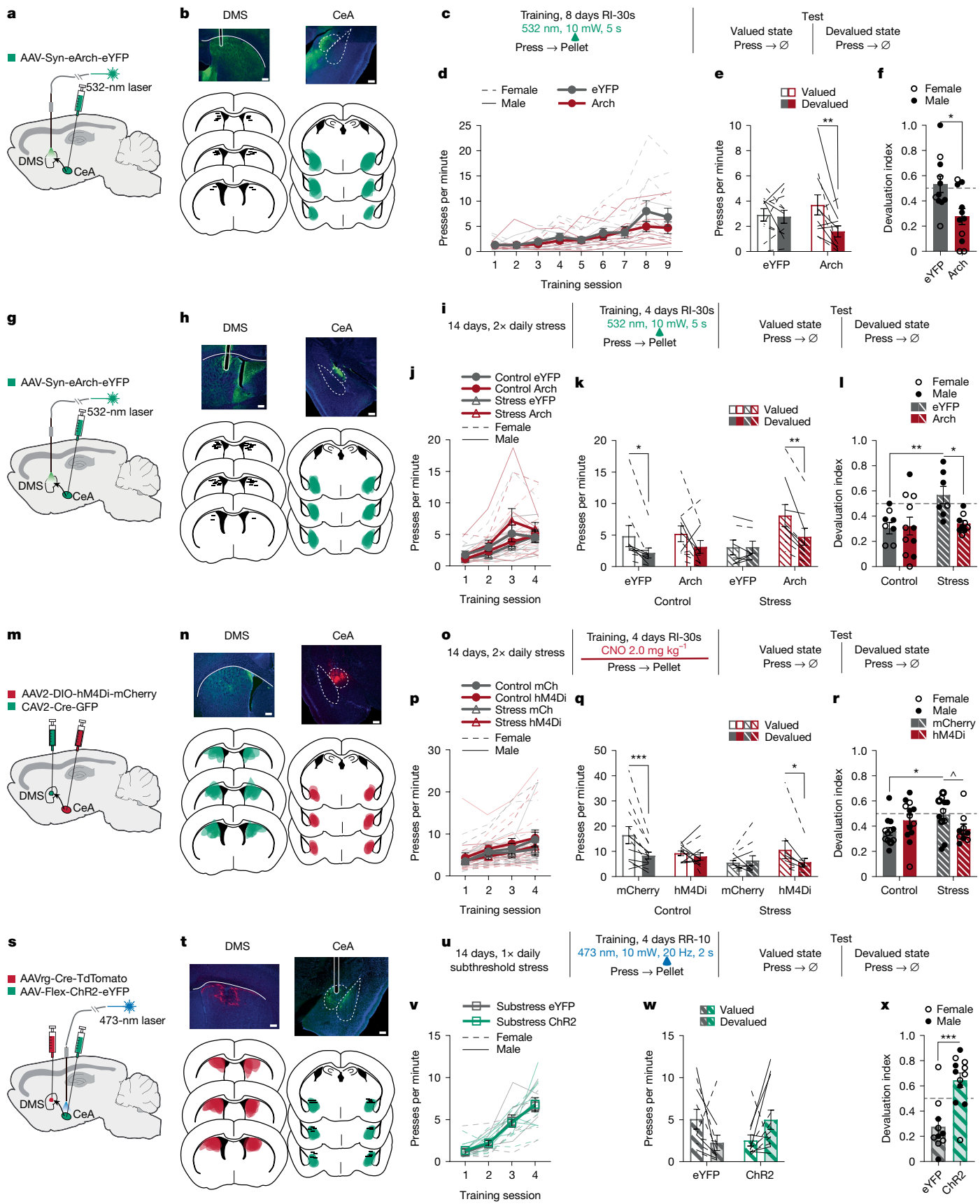


Fig. 4 | See next page for caption.

Fig. 4 | CeA→DMS mediates habit formation and is recruited by chronic stress to promote premature habit. **a–f**, Optogenetic inactivation of CeA→DMS projections at reward during natural habit formation. **a**, Optogenetic inhibition approach. **b**, Top, immunofluorescent images of Arch expression in CeA and optical fibre tip in the vicinity of Arch-expressing CeA terminals in the DMS. Bottom, expression and fibre map for all mice. **c**, Procedure. RI-30s, random-interval overtrain reinforcement schedule. **d**, Training press rate. Two-way ANOVA: Training $F_{1,46,29.09} = 15.69, P = 0.0001$. **e**, Devaluation test press rate. Two-way ANOVA: Virus \times Value $F_{1,20} = 4.72, P = 0.04$. **f**, Devaluation index ((Devalued presses)/(Valued presses + Devalued presses)). Two-sided *t*-test: $t_{20} = 2.80, P = 0.01$, 95% CI –0.45 to –0.06. eYFP, $n = 11$ (3 male); Arch, $n = 11$ (7 male). **g–l**, Optogenetic CeA→DMS inactivation at reward during post-stress learning. **g**, Optogenetic inhibition approach. **h**, Top, immunofluorescent images of Arch expression in CeA and optical fibre tip in the vicinity of Arch-expressing CeA terminals in the DMS. Bottom, expression and fibre map for all mice. **i**, Procedure. Stress, chronic unpredictable stress. **j**, Training press rate. Training $F_{2,15,68.91} = 31.05, P < 0.0001$. **k**, Devaluation test press rate. Three-way ANOVA: Value \times Stress \times Virus $F_{1,32} = 4.14, P = 0.05$. Control groups, two-way ANOVA: Value \times Virus $F_{1,18} = 0.15, P = 0.70$. Stress groups, two-way ANOVA: Value \times Virus $F_{1,14} = 12.88, P = 0.003$. **l**, Devaluation index. Two-way ANOVA: Stress \times Virus $F_{1,32} = 4.47, P = 0.04$. Control eYFP, $n = 9$ (5 male); Control Arch, $n = 11$ (4 male); Stress eYFP, $n = 7$ (6 male); Stress Arch, $n = 9$ (5 male). **m–r**, Chemogenetic

CeA→DMS inhibition during post-stress learning. **m**, Intersectional chemogenetic inhibition approach. **n**, Top, immunofluorescent images of retro-Cre expression in DMS. Bottom, expression map for all mice. **o**, Procedure. **p**, Training press rate. Two-way ANOVA: Training $F_{1,54,63.31} = 21.12, P < 0.0001$. **q**, Devaluation test press rate. Planned comparisons two-sided *t*-tests valued versus devalued: Control mCherry $t_{11} = 4.59, P < 0.0001$, 95% CI 4.57 to 11.73; Control hM4Di $t_{12} = 0.73, P = 0.46$, 95% CI –2.18 to 4.71; Stress mCherry $t_{10} = 0.47, P = 0.64$, 95% CI –4.62 to 2.87; Stress hM4Di $t_8 = 2.41, P = 0.02$, 95% CI 0.79 to 9.07. **r**, Devaluation index. Two-way ANOVA: Stress \times Virus $F_{1,41} = 5.99, P = 0.02$. Control mCherry, $n = 12$ (5 male); Control hM4Di, $n = 13$ (8 male); Stress mCherry, $n = 11$ (5 male); Stress hM4Di, $n = 9$ (4 male). **s–x**, Optogenetic CeA→DMS stimulation at reward during learning following subthreshold chronic stress. **s**, Intersectional optogenetic stimulation approach. **t**, Top, images of retro-Cre expression in DMS and immunofluorescent staining of Cre-dependent ChR2 expression and fibres in CeA. Bottom, expression and fibre map for all mice. **u**, Procedure. Subthreshold stress, 1× daily chronic unpredictable stress; RR-10, random-ratio reinforcement schedule. **v**, Training press rate. Two-way ANOVA: Training $F_{2,30,45.90} = 71.93, P < 0.0001$. **w**, Devaluation test press rate. Two-way ANOVA: Virus \times Value $F_{1,20} = 7.40, P = 0.01$. **x**, Devaluation index. Two-sided *t*-test $t_{20} = 4.29, P = 0.0004$, 95% CI 0.19 to 0.55. eYFP, $n = 10$ (4 male); ChR2, $n = 12$ (6 male). Data are presented as mean \pm s.e.m. $^{\wedge}P = 0.069$, $^{*}P < 0.05$, $^{**}P < 0.01$, $^{***}P < 0.001$, corrected for multiple comparisons. Scale bars, 200 μ m.

activity to disrupt action–outcome learning and, therefore, agency. Conversely, the CeA→DMS pathway mediates habit formation. Stress recruits this pathway to learning to promote the premature formation of inflexible habits. Thus, chronic stress disrupts agency and promotes habit formation by flipping the amygdala input to the DMS that supports learning.

Here we provide a model for the function of amygdala–striatal projections. Whereas the BLA→DMS pathway mediates action–outcome learning to support agency, the CeA→DMS pathway mediates the formation of routine habits. BLA→DMS pathway function in action–outcome learning is consistent with evidence that BLA lesion or BLA–DMS disconnection disrupts goal-directed behaviour^{29,48,49}. We implicate direct BLA→DMS projections. The data show that this pathway is activated by rewarding events to link rewards to the actions that earned them to enable the prospective consideration of action consequences needed for flexible decision-making. These data do not accord with evidence that BLA→DMS ablation does not disrupt action–outcome learning⁵⁰. Such ablations may allow compensatory mechanisms that are not possible with temporally specific manipulation. Unlike the BLA→DMS pathway, the CeA→DMS pathway is not typically activated during action–outcome learning. Rather CeA→DMS projections mediate the natural habit formation that occurs with repeated practice of a routine. This is consistent with evidence that CeA neurons are activated by rewards with overtraining⁴⁵, that CeA lesion disrupts habit³², and that CeA→DMS projections oppose flexible adjustment of behaviour when an action is no longer rewarded³⁵. Unlike valence-processing models of amygdala function^{51,52}, our data indicate that BLA and CeA projections to the DMS are unlikely to convey simple positive or negative valence, but rather differentially shape the content of learning. The data support a parallel model⁵³, whereby, by means of distinct outputs to the DMS, the amygdala actively gates the nature of learning to regulate the balance of behavioural control strategies. An important question raised by this model is how different reward learning experiences, schedules of reinforcement, and training regimes recruit activity in these pathways and how this intersects with stress and other life experiences.

Stressful life events can disrupt one's agency and promote the formation of inflexible, potentially maladaptive, habits. Indeed, after chronic stress, people become less able to adapt their behaviour when its outcome has been devalued^{1–5}. Using two independent tests, we provide evidence in male and female mice that a recent history of chronic stress disrupts the action–outcome knowledge needed for agency

and instead causes the formation of inflexible habits. Habit formation in stressed mice was premature. Whereas we showed habits formed naturally with overtraining on an RI schedule, stressed mice form habits with only a limited amount of such training. Stress disrupts agency and promotes habit regardless of whether behaviour is reinforced on the agency-promoting RR schedule or the habit-promoting RI schedule. We found that chronic stress disrupts action–outcome learning and promotes habit formation by flipping the activity of BLA and CeA inputs to the DMS.

Chronic stress attenuates reward-learning-related activity in the BLA→DMS pathway to disrupt action–outcome learning and agency and instead recruits activity in the CeA→DMS pathway to promote the formation of inflexible habits. That agency could be rescued by manipulations to oppose these stress effects during only the learning phase indicates that stress influences behavioural control by shaping learning. The stress-induced attenuation of BLA→DMS activity was surprising because the BLA is, generally, hyperactive following chronic stress^{54–61} (compare with ref. 62). This may suggest that the effect of stress on BLA neurons depends on their projection target. Elevated CeA→DMS activity following stress is consistent with evidence that stress increases CeA activity^{63–65}. Whereas stress attenuated BLA→DMS activity throughout learning, the CeA→DMS pathway was progressively recruited across training in stressed mice. This could indicate that stress-induced CeA→DMS engagement requires repeated reward learning or reinforcement opportunity. It could also suggest the CeA→DMS pathway is engaged to compensate for the stress-induced attenuation of the BLA→DMS pathway activity needed for action–outcome learning. Indeed, the transition of behavioural control to habit systems requires a shift in behavioural control from BLA to CeA⁶⁶. Such speculations require further evaluation of amygdala–striatal activity using dual-pathway recordings and manipulations. Activation of the CeA→DMS pathway was itself not sufficient to promote habit formation. CeA→DMS activation did, however, tip the balance towards habit following a subthreshold mild chronic stress experience. Thus, stress may prime the CeA→DMS pathway to be recruited during subsequent learning. CeA→DMS activation may work along with a confluence of disruptions, probably to the BLA→DMS pathway, but also to cortical inputs to the DMS^{5,42} to promote habit formation. The CeA can also work indirectly, probably via the midbrain^{67,68}, with the dorsolateral striatum to regulate habit formation^{32,66}. Thus, the CeA may promote habit through both direct and indirect pathways to the striatum. Although evidence from the terminal optogenetic inhibition experiments confirms the

Article

involvement of direct amygdala projections to the DMS, both pathways may collateralize and such collaterals may, too, be involved in learning and affected by stress.

The discoveries here open the door to many important future questions. One is the mechanisms through which chronic stress affects amygdala–striatal activity. That chronic stress occurred before training and did not alter spontaneous activity in either pathway, suggests it may lay down neuroplastic changes in these pathways that become influential during subsequent learning opportunities. How such changes occur is a big and important question for future research. They probably involve a combination of stress action in the amygdala, perhaps via canonical stress systems such as corticotropin-releasing hormone⁶⁹ and/or kappa/dynorphin⁷⁰, and stress action at regions upstream to the amygdala. Epigenetic mechanisms may also be involved⁷¹. An equally substantial next question is how these pathways influence downstream DMS activity. Indeed, DMS neuronal activity, especially plasticity in dopamine D1 receptor-expressing neurons⁷², is critical for the action–outcome learning that supports goal-directed decision-making and when suppressed promotes inflexible habits^{26–28}. A reasonable speculation is that the excitatory BLA→DMS pathway promotes downstream learning-related activity in the DMS to support action–outcome learning and that the inhibitory CeA→DMS pathway dampens such activity to encourage habit formation. In this regard, amygdala–striatal inputs may coordinate with corticostriatal inputs known to be important for supporting action–outcome learning^{5,42} and susceptible to chronic stress⁵. Both amygdala subregions and the DMS participate in drug-seeking^{66,73,74} and active-avoidance behaviour⁷⁵. The CeA is particularly implicated in compulsive drug-seeking and drug-seeking after extended use, dependence and withdrawal or stress^{66,76}. Thus, more broadly, our results indicate chronic stress could oppositely modulate BLA→DMS and CeA→DMS pathways to promote maladaptive drug-seeking and/or avoidance habits. Towards this end, whether individual differences in BLA→DMS and/or CeA→DMS activity confer resilience or susceptibility to stress-potentiated habit formation is an important future question.

Adaptive decision-making often requires understanding your agency in a situation. Knowing that your actions can produce desirable or undesirable consequences and using this to make thoughtful, deliberate, goal-directed decisions. Chronic stress can disrupt agency and promote inflexible, habitual control over behaviour. We found that stress does this with a one–two punch to the brain. Chronic stress dials down the BLA→DMS pathway activity needed to learn the association between an action and its consequence to enable flexible, well-informed decisions. It also dials up activity in the CeA→DMS pathway, causing the formation of rigid, inflexible habits. These data provide neuronal circuit insights into how chronic stress shapes how we learn and, thus, how we decide. This helps us understand how stress can lead to the disrupted decision-making and pathological habits that characterize substance use disorders and mental illness.

Online content

Any methods, additional references, Nature Portfolio reporting summaries, source data, extended data, supplementary information, acknowledgements, peer review information; details of author contributions and competing interests; and statements of data and code availability are available at <https://doi.org/10.1038/s41586-024-08580-w>.

1. Schwabe, L. & Wolf, O. T. Stress prompts habit behavior in humans. *J. Neurosci.* **29**, 7191–7198 (2009).
2. Pool, E. R. et al. Determining the effects of training duration on the behavioral expression of habitual control in humans: a multilaboratory investigation. *Learn. Mem.* **29**, 16–28 (2022).
3. Friedel, E. et al. How accumulated real life stress experience and cognitive speed interact on decision-making processes. *Front. Hum. Neurosci.* **11**, 302 (2017).
4. Schwabe, L., Dalm, S., Schächinger, H. & Oitzl, M. S. Chronic stress modulates the use of spatial and stimulus-response learning strategies in mice and man. *Neurobiol. Learn. Mem.* **90**, 495–503 (2008).
5. Dias-Ferreira, E. et al. Chronic stress causes frontostriatal reorganization and affects decision-making. *Science* **325**, 621–625 (2009).
6. Balleine, B. W. The meaning of behavior: discriminating reflex and volition in the brain. *Neuron* **104**, 47–62 (2019).
7. Graybiel, A. M. Habits, rituals, and the evaluative brain. *Annu. Rev. Neurosci.* **31**, 359–387 (2008).
8. Dickinson, A. Actions and habits: the development of behavioural autonomy. *Phil. Trans. R. Soc. Lond. B* **308**, 67–78 (1985).
9. Redish, A. D., Jensen, S. & Johnson, A. A unified framework for addiction: vulnerabilities in the decision process. *Behav. Brain Sci.* **31**, 415–437; discussion 437–487 (2008).
10. Vandaele, Y. & Ahmed, S. H. Habit, choice, and addiction. *Neuropsychopharmacology* **46**, 689–698 (2021).
11. Voon, V. et al. Disorders of compulsion: a common bias towards learning habits. *Mol. Psychiatry* **20**, 345–352 (2015).
12. Belin, D., Belin-Rauscent, A., Murray, J. E. & Everett, B. J. Addiction: failure of control over maladaptive incentive habits. *Curr. Opin. Neurobiol.* **23**, 564–572 (2013).
13. Hogarth, L., Balleine, B. W., Corbit, L. H. & Killcross, S. Associative learning mechanisms underpinning the transition from recreational drug use to addiction. *Ann. N. Y. Acad. Sci.* **1282**, 12–24 (2013).
14. Ray, L. A. et al. Capturing habitualness of drinking and smoking behavior in humans. *Drug Alcohol Depend.* **207**, 107738 (2020).
15. Gillan, C. M. et al. Disruption in the balance between goal-directed behavior and habit learning in obsessive-compulsive disorder. *Am. J. Psychiatry* **168**, 718–726 (2011).
16. Horstmann, A. et al. Slave to habit? Obesity is associated with decreased behavioural sensitivity to reward devaluation. *Appetite* **87**, 175–183 (2015).
17. Morris, R. W., Cyron, C., Green, M. J., Le Pelley, M. E. & Balleine, B. W. Impairments in action–outcome learning in schizophrenia. *Transl. Psychiatry* **8**, 54 (2018).
18. Griffiths, K. R., Morris, R. W. & Balleine, B. W. Translational studies of goal-directed action as a framework for classifying deficits across psychiatric disorders. *Front. Syst. Neurosci.* **8**, 101 (2014).
19. Byrne, K. A., Six, S. G. & Willis, H. C. Examining the effect of depressive symptoms on habit formation and habit-breaking. *J. Behav. Ther. Exp. Psychiatry* **73**, 101676 (2021).
20. Alvares, G. A., Balleine, B. W. & Guastella, A. J. Impairments in goal-directed actions predict treatment response to cognitive-behavioral therapy in social anxiety disorder. *PLoS ONE* **9**, e94778 (2014).
21. Alvares, G. A., Balleine, B. W., Whittle, L. & Guastella, A. J. Reduced goal-directed action control in autism spectrum disorder. *Autism Res.* **9**, 1285–1293 (2016).
22. Agid, O., Kohn, Y. & Lerer, B. Environmental stress and psychiatric illness. *Biomed. Pharmacother.* **54**, 135–141 (2000).
23. Baumeister, D., Lightman, S. L. & Pariante, C. M. The interface of stress and the HPA axis in behavioural phenotypes of mental illness. *Curr. Top. Behav. Neurosci.* **18**, 13–24 (2014).
24. Brady, K. T. & Sirna, R. Co-occurring mental and substance use disorders: the neurobiological effects of chronic stress. *Am. J. Psychiatry* **162**, 1483–1493 (2005).
25. Duffing, T. M., Greiner, S. G., Mathias, C. W. & Dougherty, D. M. Stress, substance abuse, and addiction. *Curr. Top. Behav. Neurosci.* **18**, 237–263 (2014).
26. Malvaez, M. & Wassum, K. Regulation of habit formation in the dorsal striatum. *Curr. Opin. Behav. Sci.* **20**, 67–74 (2018).
27. Balleine, B. W. & O'Doherty, J. P. Human and rodent homologies in action control: corticostriatal determinants of goal-directed and habitual action. *Neuropsychopharmacology* **35**, 48–69 (2010).
28. Yin, H. H., Ostlund, S. B., Knowlton, B. J. & Balleine, B. W. The role of the dorsomedial striatum in instrumental conditioning. *Eur. J. Neurosci.* **22**, 513–523 (2005).
29. Balleine, B. W., Killcross, A. S. & Dickinson, A. The effect of lesions of the basolateral amygdala on instrumental conditioning. *J. Neurosci.* **23**, 666–675 (2003).
30. Pan, W. X., Mao, T. & Dudman, J. T. Inputs to the dorsal striatum of the mouse reflect the parallel circuit architecture of the forebrain. *Front. Neuroanat.* **4**, 147 (2010).
31. Gowrishankar, R. et al. Endogenous opioid dynamics in the dorsal striatum sculpt neural activity to control goal-directed action. Preprint at *BioRxiv* <https://doi.org/10.1101/2024.05.20.595035> (2024).
32. Lingawi, N. W. & Balleine, B. W. Amygdala central nucleus interacts with dorsolateral striatum to regulate the acquisition of habits. *J. Neurosci.* **32**, 1073–1081 (2012).
33. Swanson, L. W. & Petrovich, G. D. What is the amygdala? *Trends Neurosci.* **21**, 323–331 (1998).
34. Wall, N. R., De La Parra, M., Callaway, E. M. & Kreitzer, A. C. Differential innervation of direct- and indirect-pathway striatal projection neurons. *Neuron* **79**, 347–360 (2013).
35. Heaton, E. C., Seo, E. H., Butkovich, L. M., Yount, S. T. & Gourley, S. L. Control of goal-directed and inflexible actions by dorsal striatal melanocortin systems, in coordination with the central nucleus of the amygdala. *Prog. Neurobiol.* **238**, 102629 (2024).
36. Moscarello, J. M. & Penzo, M. A. The central nucleus of the amygdala and the construction of defensive modes across the threat-imminence continuum. *Nat. Neurosci.* **25**, 999–1008 (2022).
37. Roozenendaal, B., McEwen, B. S. & Chattarji, S. Stress, memory and the amygdala. *Nat. Rev. Neurosci.* **10**, 423–433 (2009).
38. Dickinson, A. D., Nicholas, J. & Adams, C. D. The effect of the instrumental training contingency on susceptibility to reinforcer devaluation. *Q. J. Exp. Psychol.* **35**, 35–51 (1983).
39. Adams, C. D. & Dickinson, A. Instrumental responding following reinforcer devaluation. *Q. J. Exp. Psychol.* **33**, 109–121 (1981).
40. Hammond, L. J. The effect of contingency upon the appetitive conditioning of free-operant behavior. *J. Exp. Anal. Behav.* **34**, 297–304 (1980).
41. Malvaez, M. et al. Habits are negatively regulated by histone deacetylase 3 in the dorsal striatum. *Biol. Psychiatry* **84**, 383–392 (2018).
42. Gremel, C. M. & Costa, R. M. Orbitofrontal and striatal circuits dynamically encode the shift between goal-directed and habitual actions. *Nat. Commun.* **4**, 2264 (2013).
43. Alexander, G. M. et al. Remote control of neuronal activity in transgenic mice expressing evolved G protein-coupled receptors. *Neuron* **63**, 27–39 (2009).

44. Zhu, H. et al. Cre-dependent DREADD (Designer Receptors Exclusively Activated by Designer Drugs) mice. *Genesis* **54**, 439–446 (2016).
45. Amaya, K. A. et al. Habit learning shapes activity dynamics in the central nucleus of the amygdala. Preprint at *BioRxiv* <https://doi.org/10.1101/2024.02.20.580730> (2024).
46. Tipps, M., Marron Fernandez de Velasco, E., Schaeffer, A. & Wickman, K. Inhibition of pyramidal neurons in the basal amygdala promotes fear learning. *eNeuro* **5**, ENEURO.0272-18.2018 (2018).
47. Tuscher, J. J., Taxier, L. R., Fortress, A. M. & Frick, K. M. Chemogenetic inactivation of the dorsal hippocampus and medial prefrontal cortex, individually and concurrently, impairs object recognition and spatial memory consolidation in female mice. *Neurobiol. Learn. Mem.* **156**, 103–116 (2018).
48. Corbit, L. H., Leung, B. K. & Balleine, B. W. The role of the amygdala-striatal pathway in the acquisition and performance of goal-directed instrumental actions. *J. Neurosci.* **33**, 17682–17690 (2013).
49. Ostlund, S. B. & Balleine, B. W. Differential involvement of the basolateral amygdala and mediodorsal thalamus in instrumental action selection. *J. Neurosci.* **28**, 4398–4405 (2008).
50. Fisher, S. D., Ferguson, L. A., Bertran-Gonzalez, J. & Balleine, B. W. Amygdala-cortical control of striatal plasticity drives the acquisition of goal-directed action. *Curr. Biol.* **30**, 4541–4546.e5 (2020).
51. Namburi, P. et al. A circuit mechanism for differentiating positive and negative associations. *Nature* **520**, 675–678 (2015).
52. Tye, K. M. Neural circuit motifs in valence processing. *Neuron* **100**, 436–452 (2018).
53. Balleine, B. W. & Killcross, S. Parallel incentive processing: an integrated view of amygdala function. *Trends Neurosci.* **29**, 272–279 (2006).
54. Ugolini, A., Sokal, D. M., Arban, R. & Large, C. H. CRF1 receptor activation increases the response of neurons in the basolateral nucleus of the amygdala to afferent stimulation. *Front. Behav. Neurosci.* **2**, 2 (2008).
55. Liu, Z. P. et al. Chronic stress impairs GABAergic control of amygdala through suppressing the tonic GABA_A receptor currents. *Mol. Brain* **7**, 32 (2014).
56. Rosenkranz, J. A., Venheim, E. R. & Padival, M. Chronic stress causes amygdala hyperexcitability in rodents. *Biol. Psychiatry* **67**, 1128–1136 (2010).
57. Hetzel, A. & Rosenkranz, J. A. Distinct effects of repeated restraint stress on basolateral amygdala neuronal membrane properties in resilient adolescent and adult rats. *Neuropharmacology* **39**, 2114–2130 (2014).
58. Rau, A. R., Chappell, A. M., Butler, T. R., Ariwodola, O. J. & Weiner, J. L. Increased basolateral amygdala pyramidal cell excitability may contribute to the anxiogenic phenotype induced by chronic early-life stress. *J. Neurosci.* **35**, 9730–9740 (2015).
59. Sharp, B. M. Basolateral amygdala and stress-induced hyperexcitability affect motivated behaviors and addiction. *Transl. Psychiatry* **7**, e1194 (2017).
60. Masneuf, S. et al. Glutamatergic mechanisms associated with stress-induced amygdala excitability and anxiety-related behavior. *Neuropharmacology* **85**, 190–197 (2014).
61. Lowery-Gionta, E. G. et al. Chronic stress dysregulates amygdalar output to the prefrontal cortex. *Neuropharmacology* **139**, 68–75 (2018).
62. Blume, S. R., Padival, M., Urban, J. H. & Rosenkranz, J. A. Disruptive effects of repeated stress on basolateral amygdala neurons and fear behavior across the estrous cycle in rats. *Sci. Rep.* **9**, 12292 (2019).
63. Partridge, J. G. et al. Stress increases GABAergic neurotransmission in CRF neurons of the central amygdala and bed nucleus stria terminalis. *Neuropharmacology* **107**, 239–250 (2016).
64. He, F., Ai, H., Wang, M., Wang, X. & Geng, X. Altered neuronal activity in the central nucleus of the amygdala induced by restraint water-immersion stress in rats. *Neurosci. Bull.* **34**, 1067–1076 (2018).
65. Giovanniello, J. et al. A central amygdala-globus pallidus circuit conveys unconditioned stimulus-related information and controls fear learning. *J. Neurosci.* **40**, 9043–9054 (2020).
66. Murray, J. E. et al. Basolateral and central amygdala differentially recruit and maintain dorsolateral striatum-dependent cocaine-seeking habits. *Nat. Commun.* **6**, 10088 (2015).
67. Liu, J. et al. Differential efferent projections of GABAergic neurons in the basolateral and central nucleus of amygdala in mice. *Neurosci. Lett.* **745**, 135621 (2021).
68. Sah, P., Faber, E. S., Lopez De Armentia, M. & Power, J. The amygdaloid complex: anatomy and physiology. *Physiol. Rev.* **83**, 803–834 (2003).
69. Limoges, A., Yarur, H. E. & Tejeda, H. A. Dynorphin/kappa opioid receptor system regulation on amygdaloid circuitry: implications for neuropsychiatric disorders. *Front. Syst. Neurosci.* **16**, 963691 (2022).
70. Daviu, N., Bruchas, M. R., Moghaddam, B., Sandi, C. & Beyeler, A. Neurobiological links between stress and anxiety. *Neurobiol. Stress* **11**, 100191 (2019).
71. McEwen, B. S., Nasca, C. & Gray, J. D. Stress effects on neuronal structure: hippocampus, amygdala, and prefrontal cortex. *Neuropharmacology* **41**, 3–23 (2016).
72. Shan, Q., Ge, M., Christie, M. J. & Balleine, B. W. The acquisition of goal-directed actions generates opposing plasticity in direct and indirect pathways in dorsomedial striatum. *J. Neurosci.* **34**, 9196–9201 (2014).
73. Belin-Rauscent, A., Everitt, B. J. & Belin, D. Intrastriatal shifts mediate the transition from drug-seeking actions to habits. *Biol. Psychiatry* **72**, 343–345 (2012).
74. Corbit, L. H., Nie, H. & Janak, P. H. Habitual alcohol seeking: time course and the contribution of subregions of the dorsal striatum. *Biol. Psychiatry* **72**, 389–395 (2012).
75. Wendler, E. et al. The roles of the nucleus accumbens core, dorsomedial striatum, and dorsolateral striatum in learning: performance and extinction of Pavlovian fear-conditioned responses and instrumental avoidance responses. *Neurobiol. Learn. Mem.* **109**, 27–36 (2014).
76. Weera, M. M., Schreiber, A. L., Avegno, E. M. & Gilpin, N. W. The role of central amygdala corticotropin-releasing factor in predator odor stress-induced avoidance behavior and escalated alcohol drinking in rats. *Neuropharmacology* **166**, 107979 (2020).

Publisher's note Springer Nature remains neutral with regard to jurisdictional claims in published maps and institutional affiliations.

Springer Nature or its licensor (e.g. a society or other partner) holds exclusive rights to this article under a publishing agreement with the author(s) or other rightsholder(s); author self-archiving of the accepted manuscript version of this article is solely governed by the terms of such publishing agreement and applicable law.

© The Author(s), under exclusive licence to Springer Nature Limited 2025

Article

Methods

The key reagents used are listed in Supplementary Table 5.

Mice

We used male and female wild-type C57/Bl6J mice (Jackson Laboratories) aged 9–12 weeks at the time of surgery. Rabies tracing was conducted with *Drd1a-Cre* and *Adora2A-Cre* transgenic mice bred in-house and aged 8–16 weeks at the time of surgery. Mice were housed in a temperature (20–26 °C) and humidity (30–70%) regulated vivarium on 12:12 h reverse dark–light cycle (lights off at 7 a.m.). Behavioural experiments were performed during the dark phase. Mice were group housed in same-sex groups of three or four mice per cage before the onset of behavioural experiments and subsequently singly housed for the remainder of the experiment to facilitate food deprivation and preserve implants. Unless noted below, mice were provided with food (standard rodent chow; Lab Diet) and water ad libitum in the home cage. Mice were handled for 3–5 days before the start of behavioural training for each experiment. All procedures were conducted in accordance with the National Institutes of Health (NIH) Guide for the Care and Use of Laboratory Animals and were approved by the UCLA Institutional Animal Care and Use Committee.

Surgery

Mice were anaesthetized with isoflurane (3% induction, 1% maintenance) and positioned in a digital stereotaxic frame (Kopf). Subcutaneous Rimadyl (carprofen, 5 mg kg⁻¹; Zoetis) was given pre-operatively for analgesia and anti-inflammatory purposes. Small cranial holes (1–2 mm²) were drilled, through which virus or fluorescent tracers were delivered via a guide cannula (DMS: 28 G, BLA/CeA: 33 G; Plastics-One) connected to a 1-ml syringe (Hamilton Company) by intramedic polyethylene tubing (BD) and controlled by a syringe pump (Harvard Apparatus). Coordinates (Bregma) were determined using a mouse brain reference atlas⁷⁷ and were as follows: CeA, anterior–posterior (AP) −1.2, medial–lateral (ML) ±2.8, dorsal–ventral (DV) −4.6 mm; BLA, AP −1.5, ML ±3.2, DV −5.0 mm; DMS, AP +0.2, ML ±1.8, DV −2.65 mm. Virus or tracers were infused at a rate of 0.1 µl min⁻¹ and cannulae were left in place for at least 10 min post-injection. For injection-only surgeries, the skin was re-closed with Vettbond tissue adhesive (3M). For surgeries requiring fibre-optic cannulae, fibres were placed 0.3 mm above the target region for optogenetic experiments and at the infusion site for fibre photometry experiments, secured to the skull using RelyX Unicem Universal Self-Adhesive Resin (3M) and a head cap was created using C&B Metabond quick adhesive cement system (Parkell Inc.), followed by opaque dental cement (Lang Dental Manufacturing). After surgery, mice were kept on a heating pad maintained at 35 °C for 1 h and then single-housed in a new home cage for recovery and monitoring. Mice received chow containing the antibiotic trimethoprim sulfadiazine for 7 days following surgery to prevent infection, after which they were returned to standard rodent chow. Specific surgical details for each experiment are described below. In all cases, surgery occurred before the onset of stress or behavioural training.

Chronic mild unpredictable stress

The chronic mild unpredictable stress ('stress') procedure was modified from refs. 5,77–80. Mice assigned to the stress group were exposed to two stressors per day (foot shock, physical restraint, tilted cage, white noise, continuous illumination or damp bedding) for 14 days in a pseudo-randomized manner at variable time onset and for varying durations between 2 and 16 h. Each stress protocol was consistent across mice in a cohort. Control mice received equated daily handling in the vivarium by the experimenter administering the stress. Stress was administered in a separate, enclosed laboratory space distinct from both the vivarium and behavioural testing rooms. Stressed mice had home-cage nesting material removed for the duration of the stress

exposure⁸¹. Mice were transported to the stress space in individual 16-oz clear polyethylene containers and on a dedicated transport cart and placed in individual cages in the stress space. Stress efficacy was assessed by daily body weight measurements⁸². Subthreshold stress exposure was identical to stress except mice received only one stressor per day. An example stress protocol is provided in Supplementary Table 6.

Stressors. Footshock. Mice were placed in the conditioning chamber for 2 min to acclimate and then exposed to five, 2–3-s, 0.7-mA footshocks with a variable intertrial interval averaging 60 s (30–90-s range). The footshock chamber had a similar grid floor to the behavioural testing chambers (described below) but was otherwise distinct in wall shape (round), pattern (monochrome polka dot), lack of bedding, scent (75% ethanol) and lighting (off). The chambers also lacked food ports and levers. Chambers were cleaned with 75% ethanol between animals.

Physical restraint. Mice were immobilized in modified 50-ml polypropylene conical tubes with four air holes per side, one at the top and one in the cap for the tail (ten in total). Mice were scruffed and placed inside the conical tube for 2 h in their stress cage.

Tilted cage. Stress cages were placed on chocks to tilt each cage at an angle of approximately 45° for 6–16 h.

White noise. White noise (100 dB) was played in the stress space for all stressed mice for a duration of 6–16 h.

Continuous illumination. Overhead lights were turned on during the dark phase of the light cycle (7 a.m. to 7 p.m.).

Damp bedding. Approximately 200 ml of water was mixed with the stress cage corn cob bedding. Mice were placed in their stress cage with this damp bedding for 6–16 h. Mice were returned to a new home cage with clean, dry bedding afterwards.

Corticosterone enzyme-linked immunosorbent assay. Male (*n* = 11) and female (*n* = 12) mice were used for corticosterone measurements of blood serum after exposure to 0, 1 or 2 stressors per day for 14 days. Measurements were taken 24 h after the final stress exposure. Mice were decapitated and trunk blood was collected in 1.7-ml sample tubes on ice. Tubes were centrifuged at 2,000g for 10 min at 4 °C. Clear supernatant was collected and placed in new 1.7-ml sample tubes and frozen at −20 °C. Samples were diluted 1:40 in sample dilution buffer. Serum corticosterone levels were assessed using a Corticosterone ELISA kit as directed (Enzo Biosciences) and quantified on a microplate reader (Molecular Devices).

Behavioural procedures

Instrumental conditioning and tests. Instrumental conditioning procedures were adapted from our previous work⁴¹.

Apparatus. Training took place in Med Associates wide mouse conditioning chambers (East Fairfield, VT, USA) housed in sound- and light-attenuating boxes. Each chamber had metal grid floors and contained a retractable lever to the left of a recessed food delivery port (magazine) on the front wall. A photobeam entry detector was positioned at the entry to the food port. Each chamber was equipped with two pellet dispensers to deliver either 20-mg grain or chocolate-flavoured purified pellets (Bio-Serv) into the food port. A fan mounted to the outer chamber provided ventilation and external noise reduction. A 3 W, 24 V house light mounted on the top of the back wall opposite the food port provided illumination. To monitor animal behaviour, monochrome digital cameras (Med Associates) were positioned over the top of the conditioning chambers. For optogenetic manipulations, chambers were outfitted with an Intensity Division Fiberoptic Rotary Joint (Doric Lenses) connecting the output fibre-optic patch cords to a 473 or 593-nm laser (Dragon Lasers) positioned outside the chamber.

Food deprivation. At 3–5 days before the start of behavioural training, mice were food-deprived to maintain 85–90% of their free-feeding body weight. Mice were given 1.5–3.0 g of their home chow at the same

time daily at least 2 h after training sessions. For experiments involving stress, food deprivation began during the last 3 days of the stress procedure. Owing to food deprivation, body weights did not differ between groups at the start or end of training (Supplementary Table 2).

Outcome pre-exposure. To familiarize mice with the food pellet that would become the instrumental outcome, mice were given one session of outcome pre-exposure. Mice were placed in a clean, empty cage and allowed to consume 20–30 of the food pellets from a metal cup. If any pellets remained, they were placed in the home cage overnight for consumption.

Magazine conditioning. Mice received one session of training in the operant chamber to learn where to receive the food pellets (grain or chocolate-purified pellets each weighing 20 mg). Mice received 20–30 non-contingent pellet deliveries from the food port with a fixed 60-s intertrial interval.

Instrumental conditioning. Mice received four sessions (one session per day consecutively), minimum, of instrumental conditioning in which lever presses earned delivery of a single food pellet. Earned pellet type (grain or chocolate) was counterbalanced across mice within each group of each experiment. Each session began with illumination of the house light and extension of the lever, and ended with retraction of the lever and turning off of the house light. Sessions ended after the total available outcomes (20 or 30, as noted for each experiment below) had been earned or a maximum time limit (20 or 30 min, as noted below) had been reached. In all cases, training began on a fixed-ratio 1 schedule (FR-1), in which each action was reinforced with one food pellet. Once mice completed two sessions in which they earned 80% of the maximum outcomes, the reinforcement schedule was escalated to either RI or RR as described for each experiment below. For the RI protocol, mice received one session on an RI-15s schedule then two or three sessions on the final RI-30s schedule (variable average 15- or 30-s interval must elapse following a reinforcer for another press to be reinforced). Mice on the RR protocol received one session each of RR-2, RR-5 and RR-10 schedule of reinforcement (variable press requirement average of two, five or ten presses to earn the food pellet). For the overtraining protocol, mice received eight total training sessions, one on an RI-15s schedule then seven sessions on the final RI-30s schedule.

For mice in the contingency degradation experiment, following FR-1 training, they received two days of training in which each press was reinforced with a probability of 0.2 ($P(\text{Reward} \mid \text{Press}) = 0.2$) and a final session in which each press earned reward with a probability of 0.1 ($P(\text{Reward} \mid \text{Press}) = 0.1$).

Alternate outcome exposures. To equate exposure to the non-trained pellet, all mice were given non-contingent access to the same number of alternate food pellets (for example, chocolate pellets if grain pellets served as the training outcome) as the earned pellet type in a different context (clear plexiglass cage) a minimum of 2 h before or after (alternated daily) each RI or RR instrumental training session.

Sensory-specific satiety-outcome-devaluation test. Testing began 24 h after the final instrumental conditioning session. Mice were given 1–1.5 h access to either 4 g of the food pellets previously earned by lever pressing (Devalued condition) or 4 g of the non-trained pellets to control for general satiety (Valued condition). The remaining pellets were weighed following prefeeding to measure total consumption. Consumption did not differ significantly between the Devalued and Valued conditions for any experiment (Supplementary Table 3). Immediately after this prefeeding, lever pressing was assessed during a 5-min non-reinforced probe test. Following the probe test, mice were given a 10-min consumption choice test with simultaneous access to 1 g of both pellet types to ensure rejection of the devalued outcome. In all cases, mice consumed less of the prefed pellet than non-prefed pellet, indicating successful sensory-specific satiety devaluation (Supplementary Table 4). Twenty-four hours after the first devaluation test, mice received one session of instrumental retraining on the final reinforcement schedule (RI-30 or RR-10), followed the next day by a

second devaluation test in which they were prefed the opposite food pellet. Thus, each mouse was tested in both the Valued and Devalued conditions, with test order counterbalanced across mice in each group for each experiment.

Contingency degradation test. Twenty-four hours after the final instrumental conditioning session, mice received a 20-min contingency degradation session during which lever pressing continued to earn a reward with a probability of 0.1, but a reward was also delivered freely with the same probability even if mice did not press the lever (non-contingent; $(P(\text{Reward} \mid \text{Press}) = 0.1, P(\text{Reward} \mid \text{NoPress}) = 0.1)$). Thus, lever pressing was no longer necessary to earn a reward. This session was identical for non-degraded controls, except they did not receive non-contingent rewards ($P(\text{Reward} \mid \text{Press}) = 0.1, P(\text{Reward} \mid \text{NoPress}) = 0$). Twenty-four hours following the contingency degradation session, the effects of this contingency change were assessed in a 5-min non-reinforced probe test.

Real-time place preference/avoidance test. The procedure was conducted as described previously⁸³. Mice were habituated to a two-sided opaque plexiglass chamber (20 × 42 × 27 cm) for 10 min, during which their baseline preference for the left or right side of the chamber was measured. During the first 10-min test session, one side of the chamber was assigned to the light-delivery side (counterbalanced across mice within each group). Mice were placed in the non-stimulation side to start the experiment. Light (Dragon Laser) was delivered on entry into the light-paired side and continued until the mouse exited that side (optical stimulation: 473 nm, 5-ms pulse width, 20 Hz, approximately 8–10 mW at fibre tip; optical inhibition: 593 nm, continuous, approximately 8–10 mW). Mice then received a second test, identical to the first, in which the opposite side of the chamber served as the light-paired side. Sessions were video-recorded using a charged-coupled device (CCD) camera. This camera interfaced with Biobserve software (Biobserve GmbH) and a Pulse Pal (Sanworks), to track mouse position in real time and trigger laser delivery. The apparatus was cleaned with 75% ethanol after each session. Distance travelled, movement velocity and time spent in each chamber were generated using Biobserve software post-session. Time spent in laser-paired chamber was compared between groups to assess preference or aversion of laser delivery.

Open field test. The procedure was conducted as described previously⁸³. Mice were placed in an opaque plexiglass arena (34 × 34 × 34 cm) for a single 10-min session. Sessions were video-recorded using a CCD camera interfaced with Anymaze (Stoelting Co.) software, which was used to track mouse position in real time. The centre region was defined as the innermost one-third of the floor area. Brightness above the open field test was roughly 70 lux. The apparatus was cleaned with 75% ethanol after each mouse. Distance travelled, movement velocity and time spent in either centre or surrounding outer area were generated by Anymaze software and compared between groups.

Light-dark emergence test. The dark side of a two-chamber apparatus was made of black opaque plexiglass and completely enclosed except for a small entry through the middle divider. The light side was made of white opaque plexiglass and was open to the light above. Brightness in the light chamber was around 70 lux. Mice were placed in the open portion of the apparatus to initiate a 10-min session. Each session was video-recorded using a CCD camera, which interfaced with Anymaze software to track mouse location. The apparatus was cleaned with 75% ethanol after each session. Distance travelled, movement velocity and time spent in the light chamber were generated using Anymaze software and compared between groups.

Elevated plus maze. The procedure was conducted as described previously⁸⁴. The dimensions of the elevated plus maze (EPM) arms were 30 × 7 cm, and the height of the closed arm walls was 20 cm. The maze

Article

was elevated 65 cm from the floor and was placed in the centre of the behaviour room away from other stimuli. The brightness above the EPM was approximately 70 lux. For the 10-min EPM test, mice were placed in the centre of the EPM facing a closed arm. Each session was video-recorded using a CCD camera, which interfaced with Anymaze software to track mouse location in real time. The apparatus was cleaned with 75% ethanol after each session. Distance travelled, movement velocity and time spent in the centre, open arms or closed arms were generated by Anymaze software and compared between groups.

Sucrose-preference test. Mice first received habituation to two standard home-cage water bottles filled with water in the home cage for 16 h. Subsequently, one water bottle was replaced with a bottle of 10% sucrose. Bottles were left in place for 24 h and weighed before and after placement. Bottle positions were switched for another 24-h period and subsequently weighed again. Amount of sucrose and water consumed, as well as a ratio of the two, during the 48-h period was compared between groups.

Progressive ratio test. Mice were trained on the instrumental training protocol described above to a reinforcement schedule of RR-10. They were then given a progressive ratio test in which the number of lever presses required to receive a pellet increased by four with each reinforcer delivered (for example, 1, 5, 9, 13, 17, 21). The session ended after a break of more than 5 min in pressing or maximum duration of 4 h. Session duration, rewards delivered, total presses, and the break point (last completed press requirement) were collected and compared between groups.

Effects of chronic mild unpredictable stress on instrumental learning and sensitivity to outcome devaluation

Male and female (Control: final $n = 22$, 13 male; Stress: $n = 25$, 12 male) naive mice were used in this experiment to assess how a recent history of chronic stress affects instrumental learning and behavioural control strategy. Six mice (not included in the above numbers) were excluded because they did not meet instrumental training performance criteria. Mice were randomly assigned to Control and Stress groups. Mice were given 14 consecutive days of twice-daily stress or daily handling as described above. Twenty-four hours after the final stress exposure, mice began instrumental conditioning as described above. After completion of FR-1, mice received one session each of training on an RR-2, RR-5 and RR-10 reinforcement schedule (maximum 20 outcomes per 20 min per session). We chose an RR reinforcement schedule for this experiment because it tends to promote action-outcome learning and goal-directed decision-making^{38,39,42,85} and would, thus, make it more difficult for previous stress to induce habits, increasing the robustness of the results. Following training, mice received a counterbalanced set of sensory-specific satiety outcome-specific devaluation tests, as above.

Effects of chronic mild unpredictable stress on action-outcome learning

Male and female (Control Non-degraded: final $n = 7$, 3 male; Control Contingency degradation: $n = 3$, 3 male; Stress Non-degraded: $n = 7$, 3 male; Stress Contingency degradation: $n = 8$, 4 male) naive mice were used in this experiment to assess how a recent history of chronic stress affects the ability to learn an action-outcome contingency. Three mice (not included in the above numbers) were excluded because they did not meet instrumental training performance criteria. Mice were randomly assigned to Control and Stress groups. Mice were given 14 consecutive days of twice-daily stress or daily handling as described above. Twenty-four hours after the final stress exposure, mice began instrumental conditioning as described above. After completion of FR-1, mice received two sessions of training in which lever presses were reinforced with a probability of 0.2 ($P(\text{Reward} \mid \text{Press}) = 0.2$) and one session in which they were reinforced with a probability of 0.1

($P(\text{Reward} \mid \text{Press}) = 0.1$; maximum 20 outcomes per 20 min per session). Following training, mice received a single contingency degradation or non-degraded control session, as described above. This was followed the next day by a lever-pressing probe test, described above.

Effects of chronic mild unpredictable stress on common indices of anxiety- and depression-like behaviour

Male and female (Control: final $n = 12$, 6 male; Stress: $n = 12$, 6 male) naive mice were used in this experiment to assess how a recent history of chronic stress affects performance in common indices of anxiety- and depression-like behaviour. Mice were randomly assigned to Control and Stress groups. Mice were given 14 consecutive days of twice-daily stress or daily handling as described above. Twenty-four hours after the final stress exposure, mice began testing, as described above. Mice were given tests in the order: open field test, light-dark emergence test, EPM, sucrose-preference test and progressive ratio test.

Tracing

Anterograde tracing of CeA neurons was performed as described previously⁸⁶. Male ($n = 2$) and female ($n = 2$) naive mice were infused bilaterally with the anterograde tracer AAV8-Syn-mCherry (Addgene) in the CeA (0.2 μ l). Virus was allowed to express for 4 weeks, following which mice were perfused and histology was processed as described below to identify fluorescently labelled fibres in the dorsal striatum.

For retrograde tracing of DMS-projecting amygdala neurons, male ($n = 2$) and female ($n = 2$) naive mice were infused with Fluorogold (Santa Cruz Biotechnology; 4% in sterile saline) in the DMS (0.2 μ l). Virus was allowed to express for 5 days, following which mice were perfused and histology was processed as described below to identify fluorescently labelled cell bodies in the CeA and BLA.

For retrograde tracing of monosynaptic inputs onto Drd1a⁺ or A2A⁺ DMS neurons, male ($n = 4$) and female ($n = 4$) *Drd1a-cre* or male ($n = 3$) and female ($n = 2$) *Adora2A-cre* naive mice were infused with 0.3 μ l of AAV2-hSyn-FLEX-TVA-P2A-eGFP-2A-oG (Salk Gene Transfer, Targeting and Therapeutics Facility) in the DMS. Three weeks later, mice were infused with 0.3 μ l of EnvA G-deleted Rabies-mCherry at the same DMS coordinates. Mice were perfused 1 week later and tissue was processed as described below to identify monosynaptically labelled inputs in CeA and BLA. 4 *Drd1a-cre* and 1 *Adora2A-cre* mice were removed because of starter virus spillover in the bed nucleus of the stria terminalis.

Fibre photometry calcium imaging of CeA → DMS or BLA → DMS projections during instrumental learning following stress

Male and female (BLA → DMS Control: final $n = 9$, 4 male; BLA → DMS Stress: $n = 12$, 5 male; CeA → DMS Control: $n = 11$, 6 male; CeA → DMS Stress: $n = 11$, 4 male) naive mice were used in this experiment to monitor calcium fluctuations in CeA → DMS and BLA → DMS projections during instrumental conditioning after stress. Eighteen mice (not included in the above numbers) with off-target viral expression and/or fibre location were excluded from the dataset. Four mice were excluded for loss of optic fibres and/or headcaps. Four mice were excluded for missing recording data from one session. Three mice that did not complete instrumental conditioning were also excluded. Mice were randomly assigned to Virus and Stress groups. At surgery, mice received a unilateral infusion (left and right hemisphere counterbalanced across mice within each group) of a retrogradely trafficked adeno-associated virus (AAV) encoding Cre-recombinase (AAVrg-Syn-Cre-P2A-dTomato; Addgene) into the DMS (0.3 μ l) and of an AAV encoding the Cre-dependent genetically encoded calcium indicator GCaMP8s (AAV9-Syn-FLEX-GCaMP8s-GFP; Addgene) into either the CeA or BLA (0.1–0.2 μ l). Fibre-optic cannulae (length 5.0 mm (BLA) or 4.6 mm (CeA), 200- μ m diameter, 0.37 numerical aperture (NA); Inper) were implanted over the GCaMP infusion site for calcium imaging at cell bodies. Mice were given 1–2 weeks to recover post-surgery, followed by 14 consecutive days of twice-daily stress or daily handling

as described above. Mice were habituated to restraint during the final 3 days of the stress or handling period. Twenty-four hours after the final stress exposure, mice began instrumental conditioning as described above. Each session began with a 3-min baseline period before the start of the instrumental session for assessment of changes in baseline calcium activity. After completion of FR-1, mice received one session each of training on an RR-2, RR-5 and RR-10 reinforcement schedule (maximum 20 outcomes per 20 min per session).

Fibre photometry was used to image bulk calcium activity in CeA→DMS or BLA→DMS neurons for 3 min before and throughout each instrumental conditioning session using a commercial fibre photometry system (Neurophotometrics Ltd). Two light-emitting diodes (470 nm: Ca²⁺-dependent GCaMP fluorescence; 415 nm: autofluorescence, motion artefact, Ca²⁺-independent GCaMP fluorescence) were reflected off dichroic mirrors and coupled via a patch cord (200 μm; 0.37 NA, Inper) to the implanted optical fibre. The intensity of excitation light was adjusted to around 100 μW at the tip of the patch cord. Fluorescence emission was passed through a 535-nm bandpass filter and focused on the complementary metal-oxide semiconductor camera sensor through a tube lens. Samples were collected at 20 Hz interleaved between the 415 and 470-nm excitation channels using a custom Bonsai workflow. Time stamps of task events were collected simultaneously through an extra synchronized camera aimed at the Med Associates interface, which sent light pulses coincident with task events (onset, press, entry, reward). Signals were saved using Bonsai software and exported to MATLAB (MathWorks) for analysis.

To assess the response to appetitive and aversive stimuli and provide a positive signal control, fibre photometry measurements were made during subsequent non-contingent reward and footshock sessions. In the first session, mice received ten non-contingent food pellet deliveries with a variable 60-s intertrial interval. Twenty-four hours later, they received a session of five, 2-s, 0.7-mA footshocks with a variable 60-s intertrial interval. Calcium signal was aligned to reward collection or shock onset using timestamps collected as above. Mice were then perfused and brain tissue was processed with standard histology procedures described below to assess viral expression location and/or spread and fibre location.

Fibre photometry analysis. Data were pre-processed using a custom-written pipeline in MATLAB (MathWorks) as described previously⁸⁷. The 415 and 470-nm signals were fit using an exponential curve. Change in fluorescence ($\Delta f/f$) at each time point was calculated by subtracting the fitted 415-nm signal from the 470-nm signal and normalizing to the fitted 415-nm data ((470 – fitted 415)/fitted 415)). The $\Delta f/f$ data were Z-scored to the average of the whole session (($\Delta f/f$ – mean $\Delta f/f$)/s.d. ($\Delta f/f$)). Z-scored traces were then aligned to behavioural event timestamps throughout each session. Area under the curve (AUC) was calculated for each individual aligned trace in each session using a trapezoidal function. We use the 3-s period before initiating presses to quantify activity related to the initiation of actions. We used the 3-s period following reward collection to quantify activity related to the earned reward and unpredicted reward. We used the 1-s period following shock onset to quantify acute shock responses and the 2-s post-shock period to quantify activity following the shock. Quantifications and signal aligned to events were averaged across trials in a session and compared across sessions and between groups. Spontaneous activity was recorded during a 3-min baseline period in the instrumental training context before each training session. Calcium events were identified as described previously⁸⁸. We defined a series of sliding-moving windows (15-s window, 1-s step) along the trace in which we filtered out high-amplitude events (more than 2× the median of the 15-s window) and calculated the median absolute deviation of the resultant trace. Calcium transients with local maxima more than 2× above the median absolute deviation were selected as events. These events were used to calculate spontaneous event frequency and amplitude for BLA→DMS and CeA→DMS pathways.

Optogenetic inhibition of BLA→DMS projections during instrumental learning

Male and female (enhanced yellow fluorescent protein (eYFP); final $n = 10$, 5 male; Arch; $n = 11$, 5 male) naive mice were used in this experiment to assess the necessity of BLA→DMS projection activity at outcome experience during training for the action–outcome learning that supports goal-directed decision-making. Thirteen mice with off-target viral expression or fibre location and six mice that did not complete instrumental conditioning were excluded from the dataset. Mice were randomly assigned to the Virus group. At surgery, mice received bilateral infusion of an AAV encoding the inhibitory opsin Arch (AAVDJ-Syn-eArch-YFP, Stanford Vector Core) or fluorophore control (AAVDJ-Syn-eYFP; Addgene) into the BLA (0.1–0.2 μl). Fibre-optic cannulae (2.5-mm length, 100-μm diameter, 0.22 NA, Inper) were implanted over the DMS. Mice were given 3 weeks to recover and allow for viral expression. Mice were habituated to restraint for attaching optical fibres for 3 days immediately before instrumental conditioning. During instrumental conditioning, mice were tethered to a 100-μm-diameter fibre-optic bifurcated patch cord (Inper) attached to a 593-nm laser (Dragon Laser) via a rotary joint. Mice were habituated to the tether during the magazine training session, but no laser was delivered. Beginning with the first FR-1 session, all mice received laser delivery during reward collection (first magazine entry after reward delivery; 5-s pulse, 8–10 mW). After completion of FR-1, mice received one session each of instrumental conditioning on an RR-2, RR-5 and RR-10 reinforcement schedule (maximum 20 outcomes per 20 min per session). We chose an RR schedule of reinforcement for this experiment because this tends to promote action–outcome learning and goal-directed decision-making^{38,39,42,85} and, thus, would make it more difficult to neurobiologically induce habit formation, increasing the robustness of the results. Following training, mice received a counterbalanced set of sensory-specific satiety outcome-specific devaluation tests, as above. Mice were tethered but no laser was delivered on test days. Mice received laser as in training during the intervening retraining session. After instrumental training and testing, mice were tested in the real-time place preference (RTPP) test as described above. Mice were then perfused and brain tissue was processed using the standard histology procedures described below to assess viral expression location and/or spread and fibre placement.

Optogenetic activation of BLA→DMS projections during instrumental learning following stress

Male and female (Control, eYFP; final $n = 11$, 7 male; Control, ChR2; $n = 7$, 4 male; Stress, eYFP; $n = 9$, 2 male; Stress, ChR2; $n = 10$, 3 male) mice were used in this experiment to assess whether activation of BLA→DMS projections during learning is sufficient to rescue action–outcome learning for goal-directed decision-making in mice with a history of stress. Four mice with off-target viral expression or fibre location and two mice that did not complete instrumental conditioning were excluded from the dataset. Mice were randomly assigned to Virus and Stress groups. At surgery, mice received a bilateral infusion of a retrogradely trafficked AAV encoding Cre-recombinase (AAVrg-Syn-Cre-P2A-dTomato; Addgene) into the DMS (0.3 μl) and AAV encoding the Cre-inducible excitatory opsin ChR2 (AAV8-Syn-DIO-ChR2-eYFP; Stanford Vector Core) or fluorophore control (AAV8-Syn-DIO-eYFP; Stanford Vector Core) into the BLA (0.1–0.2 μl). Fibre-optic cannulae (5.0-mm length, 100-μm diameter, 0.22 NA; Inper) were implanted over the BLA. Mice were given 1–2 weeks to recover post-surgery, followed by 14 consecutive days of twice-daily stress or daily handling as described above. Mice were habituated to restraint for attaching optical fibres during the final 3 days of the stress or handling period. Twenty-four hours after the final stress exposure, mice began instrumental conditioning, as described above. During instrumental conditioning, mice were tethered to a 100-μm diameter fibre-optic bifurcated patch cord (Inper)

Article

attached to a 473-nm laser (Dragon Laser) via a rotary joint. Mice were habituated to the tether during the magazine training session, but no laser was delivered. Beginning with the first FR-1 session, all animals received laser delivery during reward collection (first magazine entry after reward delivery; 2-s duration, 20 Hz, 5-ms pulse width, 8–10 mW). After completion of FR-1, mice received one training session on an RI-15s reinforcement schedule and two training sessions on the RI-30s schedule (maximum 20 outcomes per 20 min per session). We chose an RI reinforcement schedule for this experiment because it tends to promote habit formation^{38,39,42,85} and, thus, would make it more difficult to neurobiologically prevent stress-potentiated habit, increasing the robustness of the results. Following training, mice received a counterbalanced set of sensory-specific satiety outcome-specific devaluation tests, as above. Mice were tethered but no laser was delivered on test days. Mice received laser as in training during the intervening retraining session. Mice were then perfused and brain tissue was processed using the standard histology procedures described below to assess viral expression location and/or spread and fibre placement.

Chemogenetic activation of BLA→DMS projections during instrumental learning following stress

Male and female (Control mCherry: final $n = 12$, 7 male; Control hM3Dq: $n = 6$, 3 male; Stress mCherry: $n = 9$, 5 male; Stress hM3Dq: $n = 10$, 5 male) naive mice were used in this experiment to assess whether activation of BLA→DMS projections during learning is sufficient to rescue action–outcome learning for goal-directed decision-making in mice with a history of stress. Fifteen mice with off-target viral expression and two mice that did not complete instrumental conditioning were excluded from the dataset. Mice were randomly assigned to the Virus and Stress groups. At surgery, all mice received bilateral infusion of the retrogradely trafficked canine adenovirus encoding Cre-recombinase (CAV2-Cre-GFP; Plateforme de Vectorologie de Montpellier) into the DMS (0.3 μ l) and AAV encoding the Cre-inducible excitatory designer receptor hM3Dq (AAV2-Syn-DIO-hM3Dq-mCherry; Addgene) or fluorophore control (AAV2-Syn-DIO-mCherry; Addgene) into the BLA (0.1–0.2 μ l). Mice were given 1–2 weeks to recover post-surgery, followed by 14 consecutive days of twice-daily stress or daily handling, as described above. Mice were habituated to intraperitoneal injections during the final 3 days of the stress or handling period. Twenty-four hours after the final stress exposure, mice began instrumental conditioning, as described above. All mice received an intraperitoneal injection of CNO (water soluble, 0.2 mg kg⁻¹; Hello Bio)^{43,44,89–91} 30 min before each instrumental conditioning session. Upon completion of FR-1 (80% maximum rewards delivered), mice received one training session on the RI-15s reinforcement schedule following by two sessions on an RI-30s schedule (maximum 30 outcomes per 30 min per session). We chose an RI schedule of reinforcement for this experiment because it tends to promote habit formation^{38,39,42,85} and, thus, would make it more difficult to neurobiologically prevent stress-potentiated habit, increasing the robustness of the results. Following training, mice received a counterbalanced pair of sensory-specific satiety outcome-specific devaluation tests, as above. No CNO was given on test days. CNO was given before the retraining session (RI-30s) in between tests. After instrumental training and testing, mice were perfused and brain tissue was processed using the standard histology procedures described below to assess viral expression location and spread.

Optogenetic inactivation of CeA→DMS projections during instrumental overtraining

Male and female (Control eYFP: $n = 11$, 3 male; Control Arch: $n = 11$, 7 male) naive mice were used in this experiment to assess the necessity of CeA→DMS projection activity at outcome experience during learning for the natural habit formation that occurs with overtraining. Two mice with off-target viral expression or fibre location were excluded from the dataset. Mice were randomly assigned to the Virus

group. At surgery, mice received bilateral infusion of an AAV encoding the inhibitory opsins Arch (AAVDJ-Syn-eArch-eYFP; Stanford Vector Core) or fluorophore control (AAVDJ-Syn-eYFP; Addgene) into the CeA (0.1–0.2 μ l). Fibre-optic cannulae (2.5-mm length, 100- μ m diameter, 0.22 NA; Inper) were implanted over the DMS. Mice were given 1 week to recover post-surgery. Mice were habituated to restraint for attaching optical fibres. Mice then receive instrumental overtraining on the RI-30s schedule as described above. During instrumental conditioning, mice were tethered to a 100- μ m-diameter fibre-optic bifurcated patch cord (Inper) attached to a 593-nm laser (Dragon Laser) via a rotary joint. Mice were habituated to the tether during the magazine training session, but no laser was delivered. Beginning with the first FR-1 session, all mice received laser delivery during reward collection (first magazine entry after reward delivery; 5-s pulse, 8–10 mW). After completion of FR-1, mice received one training session on an RI-15s reinforcement schedule and seven training sessions on the RI-30s schedule (maximum 20 outcomes per 20 min per session). We chose an RI reinforcement schedule for this experiment because it tends to promote habit formation^{38,39,42,85}. We overtrained mice to also promote the formation of habits naturally in control mice. Following training, mice received a counterbalanced set of sensory-specific satiety outcome-specific devaluation tests, as above. Mice were tethered but no laser was delivered on test days. Mice received laser as in training during the intervening retraining session. Mice were then perfused and brain tissue was processed using the standard histology procedures described below to assess viral expression location and/or spread and fibre placement.

Optogenetic inactivation of CeA→DMS projections during instrumental learning following stress

Male and female (Control eYFP: $n = 9$, 5 male; Control Arch: $n = 11$, 4 male; Stress eYFP: $n = 7$, 6 male; Stress Arch: $n = 9$, 5 male) naive mice were used in this experiment to assess the necessity of CeA→DMS projection activity at outcome experience during learning for stress-potentiated habit formation. Twelve mice with off-target viral expression or fibre location and two mice that did not complete instrumental conditioning were excluded from the dataset. Mice were randomly assigned to the Virus and Stress groups. At surgery, mice received bilateral infusion of an AAV encoding the inhibitory opsins Arch (AAVDJ-Syn-eArch-eYFP; Stanford Vector Core) or fluorophore control (AAVDJ-Syn-eYFP; Addgene) into the CeA (0.1–0.2 μ l). Fibre-optic cannulae (2.5-mm length, 100- μ m diameter, 0.22 NA; Inper) were implanted over the DMS. Mice were given 1–2 weeks to recover post-surgery, followed by 14 consecutive days of twice-daily stress or daily handling as described above. Mice were habituated to restraint for attaching optical fibres during the final 3 days of the stress or handling period. Twenty-four hours after the final stress exposure, mice began instrumental conditioning as described above. During instrumental conditioning, mice were tethered to a 100- μ m-diameter fibre-optic bifurcated patch cord (Inper) attached to a 593-nm laser (Dragon Laser) via a rotary joint. Mice were habituated to the tether during the magazine training session, but no laser was delivered. Beginning with the first FR-1 session, all mice received laser delivery during reward collection (first magazine entry after reward delivery; 5-s pulse, 8–10 mW). After completion of FR-1, mice received one training session on an RI-15s reinforcement schedule and two training sessions on an RI-30s schedule (maximum 20 outcomes per 20 min per session). We chose an RI reinforcement schedule for this experiment because it tends to promote habit formation^{38,39,42,85} and, thus, would make it more difficult to neurobiologically prevent stress-potentiated habit, increasing the robustness of the results. Following training, mice received a counterbalanced set of sensory-specific satiety outcome-specific devaluation tests, as above. Mice were tethered but no laser was delivered on test days. Mice received laser as in training during the intervening retraining session. After instrumental training and testing, mice were tested in the RTPP test as described above. Mice were then perfused and brain tissue was

processed using the standard histology procedures described below to assess viral expression location and/or spread and fibre placement.

Chemogenetic inactivation of CeA→DMS projections during instrumental learning following stress

Male and female (Control mCherry: $n = 12$, 5 male; Control hM4Di: $n = 13$, 8 male; Control mCherry: $n = 11$, 5 male; Control hM4Di: $n = 9$, 4 male) naive mice were used in this experiment to assess the necessity of CeA→DMS projection activity during learning for stress-potentiated habit formation. Sixteen mice with off-target viral expression and three mice that did not complete instrumental conditioning were excluded from the dataset. Mice were randomly assigned to the Virus and Stress groups. At surgery, all mice received bilateral infusion of the retrogradely trafficked canine-adenovirus encoding Cre-recombinase (CAV2-Cre-GFP; Plateforme de Vectorologie de Montpellier) into the DMS (0.3 μ l) and AAV encoding the Cre-inducible inhibitory designer receptor human M4 muscarinic receptor (hM4DG; AAV2-Syn-DIO-hM4Di-mCherry; Addgene) or fluorophore control (AAV2-Syn-DIO-mCherry; Addgene) into the CeA (0.1–0.2 μ l). Mice were given 1–2 weeks to recover post-surgery, followed by 14 consecutive days of twice-daily stress or daily handling as described above. Mice were habituated to intraperitoneal injections during the final 3 days of the stress or handling period. Twenty-four hours after the final stress exposure, mice began instrumental conditioning as described above. All mice received an intraperitoneal injection of CNO (2 mg kg⁻¹; Hello Bio)^{46,47,89,92} 30 min before each instrumental conditioning session. Upon completion of FR-1, mice received one session of training on an RI-15s reinforcement schedule followed by two sessions on the RI-30s schedule (maximum 30 outcomes per 30 min per session). We chose an RI reinforcement schedule for this experiment because it tends to promote habit formation^{38,39,42,85} and, thus, would make it more difficult to neurobiologically prevent stress-potentiated habit, increasing the robustness of the results. Following training, mice received a counterbalanced pair of sensory-specific satiety outcome-specific devaluation tests, as above. No CNO was given on test days. CNO was given before the retraining session. After instrumental training and testing, mice were perfused and brain tissue was processed using the standard histology procedures described below to assess viral expression location and spread.

Optogenetic activation of CeA→DMS projections during instrumental learning

Male and female (eYFP: $n = 17$, 9 male; ChR2: $n = 6$, 3 male) naive mice were used in this experiment to assess whether CeA→DMS projection activation at outcome experience during learning is sufficient to promote habit formation. Eleven mice with off-target viral expression or fibre location and four mice that did not complete instrumental conditioning were excluded from the dataset. Mice were randomly assigned to the Virus group. Given the low density of CeA→DMS projections, we choose to activate DMS-projecting CeA cell bodies. At surgery, mice received a bilateral infusion of a retrogradely trafficked AAV encoding Cre-recombinase (AAVrg-Syn-Cre-P2A-dTomato; Addgene) into the DMS (0.3 μ l) and AAV encoding the Cre-inducible excitatory opsins ChR2 (AAV8-Syn-DIO-ChR2-eYFP; Stanford Vector Core) or fluorophore control (AAV8-Syn-DIO-eYFP; Stanford Vector Core) into the CeA (0.1–0.2 μ l). Fibre-optic cannulae (5.0-mm length, 100- μ m diameter, 0.22 NA; Inper) were implanted over the CeA. Mice were given 3 weeks to recover and allow for viral expression. Mice were habituated to restraint for 3 days before instrumental conditioning. During instrumental conditioning, mice were tethered to a 100- μ m-diameter fibre-optic bifurcated patch cord (Inper) attached to a 473 nm laser (Dragon Laser) via a rotary joint. Mice were habituated to the tether during the magazine training session, but no laser was delivered. Beginning with the first FR-1 session, all mice received laser delivery during reward collection (first magazine entry after reward delivery; 2-s duration, 20 Hz, 5-ms

pulse width, 8–10 mW). After completion of FR-1, mice received 1 day each of training on an RR-2, RR-5 and RR-10 reinforcement schedule (maximum 20 outcomes per 20 min per session). We chose an RR schedule of reinforcement for this experiment because it tends to promote action-outcome learning and goal-directed decision-making^{38,39,42,85} and, thus, would make it more difficult to neurobiologically induce habit formation, increasing the robustness of the results. Following training, mice received a counterbalanced set of sensory-specific satiety outcome-specific devaluation tests, as above. Mice were tethered but no laser was delivered on test days. Mice received laser as in training during the intervening retraining session. After instrumental training and testing, mice were tested in the RTPP test, as described above. Mice were then perfused and brain tissue was processed using the standard histology procedures described below to assess viral expression location and/or spread and fibre placement.

Optogenetic activation of CeA→DMS projections during instrumental learning following subthreshold stress

Male and female (eYFP: $n = 10$, 4 male; ChR2: $n = 12$, 6 male) naive mice were used in this experiment to assess whether CeA→DMS projection activation at outcome experience during learning is sufficient to promote habit formation in mice with a history of less-frequent stress (subthreshold for promoting habit formation). Eleven mice with off-target viral expression or fibre location and four mice that did not complete instrumental conditioning were excluded from the dataset. Mice were randomly assigned to the Virus groups. Similar to optogenetic activation of CeA→DMS neurons in control mice, we chose to target cell bodies with this approach. At surgery, mice received bilateral infusion of a retrogradely trafficked AAV encoding Cre-recombinase (AAVrg-Syn-Cre-P2A-dTomato; Addgene) into the DMS (0.3 μ l) and AAV encoding the Cre-inducible excitatory opsins ChR2 (AAV8-Syn-DIO-ChR2-eYFP; Stanford Vector Core) or fluorophore control (AAV8-Syn-DIO-eYFP; Stanford Vector Core) into the CeA (0.1–0.2 μ l). Fibre-optic cannulae (5.0-mm length, 100- μ m diameter, 0.22 NA; Inper) were implanted over the CeA. Mice were given 1–2 weeks to recover post-surgery, followed by 14 consecutive days of once-daily stress or daily handling as described above. Mice were habituated to restraint for attaching optical fibres during the final 3 days of the subthreshold stress or handling period. Twenty-four hours after the final stress exposure, mice began instrumental conditioning, as described above. During instrumental conditioning, mice were tethered to a 100- μ m-diameter fibre-optic bifurcated patch cord (Inper) attached to a 473-nm laser (Dragon Laser) via a rotary joint. Mice were habituated to the tether during the magazine training session, but no laser was delivered. Beginning with the first FR-1 session, all mice received laser delivery during reward collection (first magazine entry after reward delivery; 2-s duration, 20 Hz, 5-ms pulse width, 8–10 mW). After completion of FR-1, mice received 1 day each of training on an RR-2, RR-5 and RR-10 reinforcement schedule (maximum 20 outcomes per 20 min per session). Following training, mice received a counterbalanced set of sensory-specific satiety outcome-specific devaluation tests, as above. Mice were tethered but no laser was delivered on test days. Mice received laser during the intervening retraining session. After instrumental training and testing, mice were tested in the RTPP test, as described above. Mice were then perfused and brain tissue was processed using the standard histology procedures described below to assess viral expression location and/or spread and fibre placement.

Immunohistochemistry

Mice were anesthetized with isoflurane and perfused transcardially with ice-cold phosphate-buffered saline (PBS) followed by cold 4% paraformaldehyde. The brains were removed, post-fixed in 4% paraformaldehyde, then cryoprotected in 30% sucrose in PBS. Coronal slices (30 μ m) were taken on a cryostat and collected in PBS. We undertook immunohistochemical analysis as described previously^{86,87,93,94}.

Article

Briefly, floating sections were blocked for 1 h at room temperature in blocking solution (3% normal goat serum (Jackson ImmunoResearch Laboratories), 0.3% Triton X-100 (Fisher)) in PBS and then incubated overnight with gentle agitation at 4 °C in blocking solution plus a 1:1,000 dilution primary antibody (chicken anti-green fluorescent protein (GFP) polyclonal, Abcam; rabbit anti-dsRed polyclonal, Takara Bio). Sections were then incubated covered with gentle agitation for 2 h at room temperature in blocking solution plus a 1:500 dilution secondary antibody (goat anti-rabbit immunoglobulin G AlexaFluor 594 conjugate; goat anti-chicken immunoglobulin G AlexaFluor 488 conjugate; Invitrogen). All sections were washed three times for 5 min each in PBS before and after each incubation step and mounted on slides using ProLong Gold antifade reagent with DAPI (Invitrogen). All images were acquired using a Keyence (BZ-X710) microscope with ×4, ×10 and ×20 objectives (CFI Plan Apo), CCD camera and BZ-X Analyze software, and a Zeiss Confocal LSM with ×2.5 and ×20 objectives and Zeiss ZEN (blue edition) image acquisition software.

Statistics and reproducibility

Statistical analysis. Datasets were analysed by two-tailed *t*-tests, or one-, two- or three-way repeated-measures analysis of variance (ANOVA), as appropriate (GraphPad Prism v.9-11; GraphPad). For chemogenetic replications of optogenetic results, we used planned comparisons for test press rate data. Some datasets were slightly non-normally distributed. For these datasets, statistical tests were also run using non-parametric analyses and the results were highly consistent. We opted to use parametric statistics for consistency across experiments and given evidence that ANOVA is robust to slight non-normality^{95,96}. Bonferroni post hoc tests corrected for multiple comparisons were performed to clarify statistical interactions. Greenhouse–Geisser correction was applied to mitigate the influence of unequal variance between conditions. Alpha levels were set at $P < 0.05$.

Sex as a biological variable. For the initial behavioural finding, sex was included as a factor in the ANOVA and found to not significantly account for variance (no main effect of sex on lever pressing acquisition: $F_{1,43} = 0.43, P = 0.51$; devaluation test press rate: $F_{1,43} = 0.60, P = 0.44$; or devaluation index: $F_{1,43} = 0.04, P = 0.84$). Therefore, data from male and female mice were combined for analyses. For subsequent experiments, male and female mice were used in roughly equal numbers, but the number (*n*) per sex was underpowered to examine sex differences. Sex was therefore not included as a factor in statistical analyses, although individual data points are visually disaggregated by sex.

Rigour and reproducibility. Group sizes were estimated on the basis of previous work with this behavioural task⁴¹ and to ensure counterbalancing of virus, stress, pellet type and devaluation test order. Investigators were not blinded to viral or stress group because they were required to administer infusions and stress exposure. All behaviours were scored using automated software (Med Associates). Each experiment included at least one replication cohort and cohorts were balanced by Virus group, Stress group and hemisphere (for photometry recordings and tracing) before the start of the experiment. Investigators were blinded to group when performing histological validation and determining exclusions on the basis of viral spread or mistargeted implant.

Reporting summary

Further information on research design is available in the Nature Portfolio Reporting Summary linked to this article.

Data availability

All data that support the findings of this study are available from the corresponding author upon request. Source data are provided with this paper.

Code availability

Custom-written MATLAB code is available at Dryad (<https://doi.org/10.5061/dryad.2jm63xt00>)⁹⁷ and from the corresponding author upon request.

77. Franklin, K. B. J. & Paxinos, G. *The Mouse Brain in Stereotaxic Coordinates* 3rd edn (Elsevier, 2008).
78. Tye, K. M. et al. Dopamine neurons modulate neural encoding and expression of depression-related behaviour. *Nature* **493**, 537–541 (2013).
79. Cerniauskas, I. et al. Chronic stress induces activity, synaptic, and transcriptional remodeling of the lateral habenula associated with deficits in motivated behaviors. *Neuron* **104**, 899–915.e898 (2019).
80. Bavley, C. C., Fischer, D. K., Rizzo, B. K. & Rajadhyaksha, A. M. Ca,_{1.2} channels mediate persistent chronic stress-induced behavioral deficits that are associated with prefrontal cortex activation of the p25/Cdk5-glucocorticoid receptor pathway. *Neurobiol. Stress* **7**, 27–37 (2017).
81. Freymann, J., Tsai, P. P., Stelzer, H. D., Mischke, R. & Hackbarth, H. Impact of bedding volume on physiological and behavioural parameters in laboratory mice. *Lab. Anim.* **51**, 601–612 (2017).
82. Patucha-Poniewiera, A., Podkowa, K., Rafala-Ulińska, A., Brański, P. & Burnat, G. The influence of the duration of chronic unpredictable mild stress on the behavioural responses of C57BL/6J mice. *Behav. Pharmacol.* **31**, 574–582 (2020).
83. La-Vu, M. Q. et al. Sparse genetically defined neurons refine the canonical role of periaqueductal gray columnar organization. *eLife* **11**, e77115 (2022).
84. Reis, F. M. et al. Dorsal periaqueductal gray ensembles represent approach and avoidance states. *eLife* **10**, e64934 (2021).
85. Hilário, M. R., Clouse, E., Yin, H. H. & Costa, R. M. Endocannabinoid signaling is critical for habit formation. *Front. Integr. Neurosci.* **1**, 6 (2007).
86. Lichtenberg, N. T. et al. The medial orbitofrontal cortex–basolateral amygdala circuit regulates the influence of reward cues on adaptive behavior and choice. *J. Neurosci.* **41**, 7267–7277 (2021).
87. Sias, A. et al. A bidirectional corticoamygdala circuit for the encoding and retrieval of detailed reward memories. *eLife* **10**, e68617 (2021).
88. Sherathiya, V. N., Schaid, M. D., Seiller, J. L., Lopez, G. C. & Lerner, T. N. GuPPy, a Python toolbox for the analysis of fiber photometry data. *Sci. Rep.* **11**, 24212 (2021).
89. Roth, B. L. DREADDs for neuroscientists. *Neuron* **89**, 683–694 (2016).
90. Vazey, E. M. & Aston-Jones, G. Designer receptor manipulations reveal a role of the locus coeruleus noradrenergic system in isoflurane general anesthesia. *Proc. Natl Acad. Sci. USA* **111**, 3859–3864 (2014).
91. Qiu, M. H., Chen, M. C., Fuller, P. M. & Lu, J. Stimulation of the pontine parabrachial nucleus promotes wakefulness via extra-thalamic forebrain circuit nodes. *Curr. Biol.* **26**, 2301–2312 (2016).
92. Pomrenze, M. B. et al. A corticotropin releasing factor network in the extended amygdala for anxiety. *J. Neurosci.* **39**, 1030–1043 (2019).
93. Malvarez, M., Shieh, C., Murphy, M. D., Greenfield, V. Y. & Wassum, K. M. Distinct cortical–amygdala projections drive reward value encoding and retrieval. *Nat. Neurosci.* **22**, 762–769 (2019).
94. Collins, A. L. et al. Nucleus accumbens cholinergic interneurons oppose cue-motivated behavior. *Biol. Psychiatry* **86**, 388–396 (2019).
95. Schmider, E., Ziegler, M., Danay, E., Beyer, L. & Bühner, M. Is it really robust? Reinvestigating the robustness of ANOVA against violations of the normal distribution assumption. *Methodology (Gott.)* **6**, 147–151 (2010).
96. Knie, U. & Forstmeier, W. Violating the normality assumption may be the lesser of two evils. *Behav. Res. Methods* **53**, 2576–2590 (2021).
97. Giovannillo, J. et al. A dual-pathway architecture for stress to disrupt agency and promote habit. *Dryad* <https://doi.org/10.5061/dryad.2jm63xt00> (2024).
98. Monteiro, S. et al. An efficient chronic unpredictable stress protocol to induce stress-related responses in C57BL/6 mice. *Front. Psychiatry* **6**, 6 (2015).
99. Mineur, Y. S., Belzung, C. & Crusio, W. E. Effects of unpredictable chronic mild stress on anxiety and depression-like behavior in mice. *Behav. Brain Res.* **175**, 43–50 (2006).
100. Fang, X. et al. Chronic unpredictable stress induces depression-related behaviors by suppressing AgRP neuron activity. *Mol. Psychiatry* **26**, 2299–2315 (2021).
101. Gong, S. et al. Targeting Cre recombinase to specific neuron populations with bacterial artificial chromosome constructs. *J. Neurosci.* **27**, 9817–9823 (2007).
102. Valjent, E., Bertran-Gonzalez, J., Hervé, D., Fisone, G. & Girault, J. A. Looking BAC at striatal signaling: cell-specific analysis in new transgenic mice. *Trends Neurosci.* **32**, 538–547 (2009).

Acknowledgements This research was supported by NIH grant no. R01DA046679 (K.M.W.), NIH grant no. R01DA058374 (K.M.W.), NIH grant no. R01DA035443 (K.M.W.), NIH grant no. T32DA024635 (J.R.G.), NIH grant no. F32DA056201 (J.R.G.), A.P. Giannini Fellowship (J.R.G.), NIH grant no. K99MH135177 (J.R.G.), NIH grant no. TL4GM118977 (N.P.), NIH grant no. R01MH119089 (A.A.) and the Staglin Center for Behavior and Brain Sciences. UCLA Behavioral Testing Core provided space and behavioural testing equipment for the open field, elevated plus maze and light–dark emergence test.

Author contributions J.R.G. and K.M.W. conceptualized and designed the experiments, interpreted the data, and wrote the paper. J.R.G. executed all experiments and analysed the data. N.P., K.L., A. Wiener, A. Wang, C.O., H.O.U., A.L.Y., J.S.P., G.N. and G.E.V. assisted with

experiments. M.S. assisted with rabies tracing experiments with resources from A.J.S. F.M.C.V.R. assisted with RTPP experiments, with advice and resources from A.A. A.C.S. wrote initial code for photometry analysis. K.R.-A. analysed spontaneous event frequency and amplitude on photometry data. M.M. contributed to the conceptualization and design of the experiments, initially optimized the instrumental conditioning procedures and data analysis, and provided important contributions to the interpretation of the data.

Competing interests The authors declare no competing interests.

Additional information

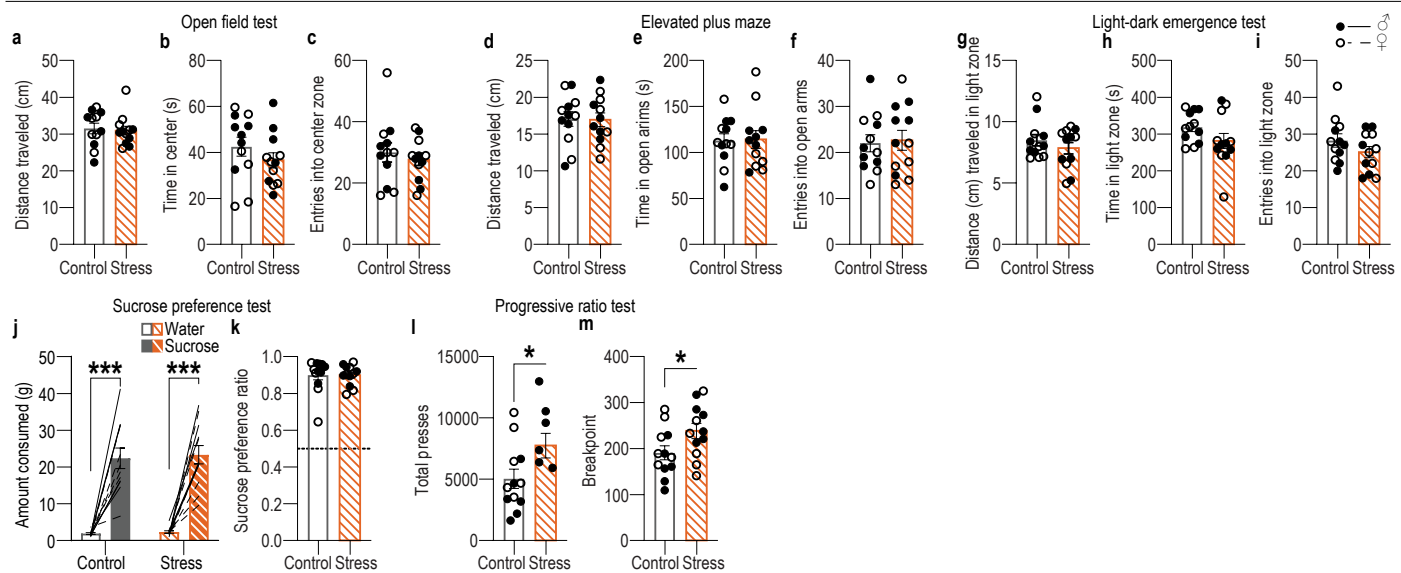
Supplementary information The online version contains supplementary material available at <https://doi.org/10.1038/s41586-024-08580-w>.

Correspondence and requests for materials should be addressed to Kate M. Wassum.

Peer review information *Nature* thanks Patricia Janak, Stephanie Groman and the other, anonymous, reviewer(s) for their contribution to the peer review of this work. Peer reviewer reports are available.

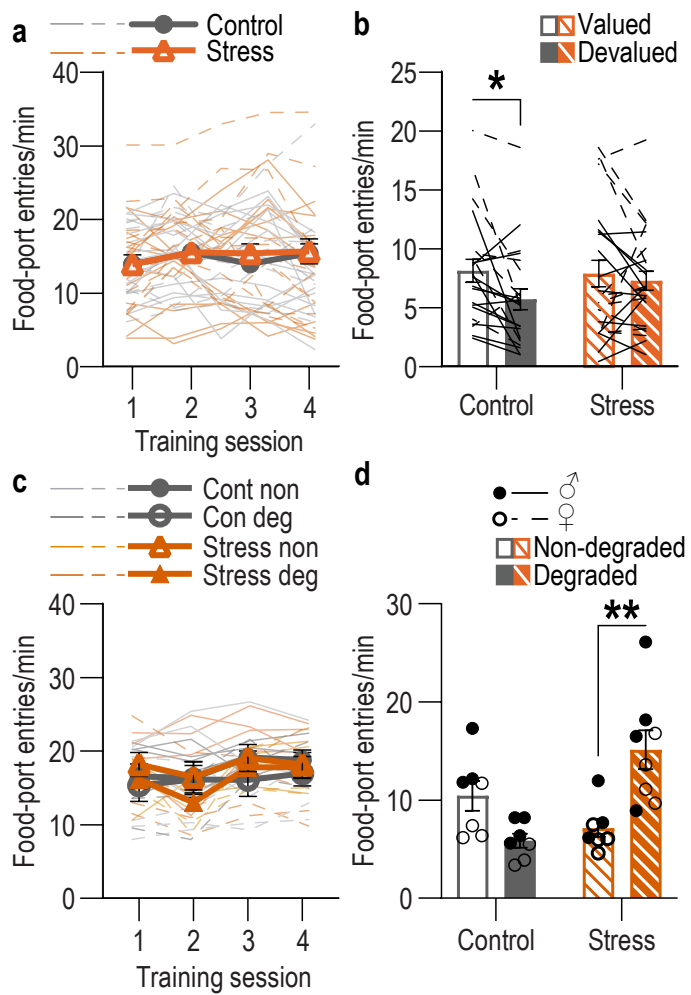
Reprints and permissions information is available at <http://www.nature.com/reprints>.

Article

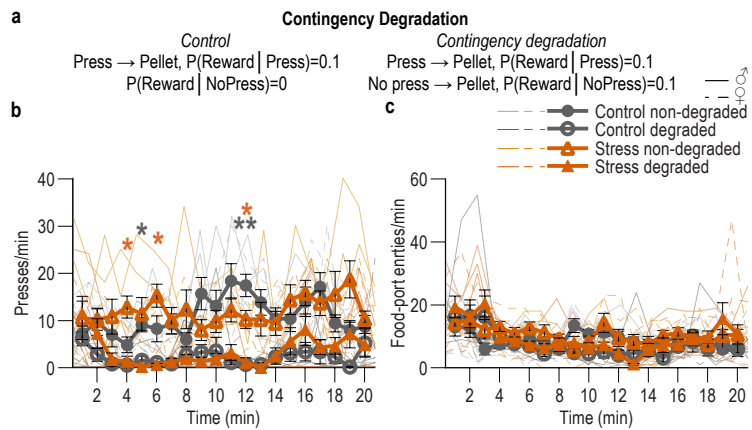


Extended Data Fig. 1 | Chronic mild unpredictable stress does not cause classic anxiety- and depression-like phenotypes. Mice received 14 consecutive d of chronic mild unpredictable stress (stress) including twice daily exposure to 1 of 6 mild stressors at pseudorandom times and orders: damp bedding (16 h), tilted cage (16 h), white noise (80 db; 2 h), continuous illumination (8 h), physical restraint (2 h), footshock (0.7-mA, 1-s, 5 shocks/10 min) prior to subsequent testing in a battery of behavioral assays classically used to assess anxiety- and depression-like behavior. (a-c) Open field test. Distance traveled (a; 2-sided t-test: $t_{(22)} = 0.32, P = 0.75, 95\% \text{ CI} -4.43 - 3.24$), time spent in center zone (b; 2-sided t-test: $t_{(22)} = 1.10, P = 0.28, 95\% \text{ CI} -16.87 - 5.16$), and entries into center zone (c; 2-sided t-test: $t_{(22)} = 0.63, P = 0.54, 95\% \text{ CI} -10.03 - 5.36$). (d-f) Elevated plus maze. Distance traveled (d; 2-sided t-test: $t_{(22)} = 0.08, P = 0.94, 95\% \text{ CI} -2.72 - 2.92$), time spent in open arms (e; 2-sided t-test: $t_{(22)} = 0.01, P = 0.92, 95\% \text{ CI} -26.17 - 23.70$), and entries into open arms (f; 2-sided t-test: $t_{(22)} = 0.23, P = 0.82, 95\% \text{ CI} -6.56 - 5.23$). (g-i) Light-dark emergence test. Distance traveled in light zone (g; 2-sided t-test: $t_{(22)} = 0.97, P = 0.34, 95\% \text{ CI} -0.73 - 2.01$), time spent in light zone (h; 2-sided t-test: $t_{(22)} = 1.57, P = 0.13, 95\% \text{ CI} -11.93 - 86.98$), and

entries into light zone (i; 2-sided t-test: $t_{(22)} = 1.37, P = 0.19, 95\% \text{ CI} -1.708 - 8.041$). (j-k) Sucrose preference test. Average amount consumed of water and 10% sucrose over 24 h (j; 2-way ANOVA: Solution: $F_{(1,22)} = 113.20, P < 0.0001$; Stress: $F_{(1,22)} = 0.14, P = 0.71$, Solution x Stress: $F_{(1,22)} = 0.02, P = 0.89$) and ratio of sucrose:water consumed (k; $t_{(22)} = 0.03, P = 0.98, 95\% \text{ CI} -0.064 - 0.063$). (l-m) Progressive ratio Tests. Total presses (l; 2-sided t-test: $t_{(22)} = 2.13, P = 0.04, 95\% \text{ CI} 172.94 - 534.6$) and breakpoint (k; Final ratio completed; 2-sided t-test: $t_{(22)} = 2.12, P = 0.46, 95\% \text{ CI} 1.02 - 94.31$). Control N = 12 (6 male), Stress N = 12 (6 male) mice. Males = closed circles, Females = open circles. Data presented as mean +/- SEM. * $P < 0.05$, ** $P < 0.001$. Our stress procedure does not affect general locomotor activity or avoidance of anxiogenic spaces or create an anhedonia phenotype. Rather this stress procedure appears to cause elevated motivation to exert effort to obtain reward. This contrasts with more severe, longer-lasting stress procedures, which do produce anxiety- and depression-like phenotypes in these tasks⁹⁸⁻¹⁰⁰. Thus, our stress procedure models chronic, low-level stress.

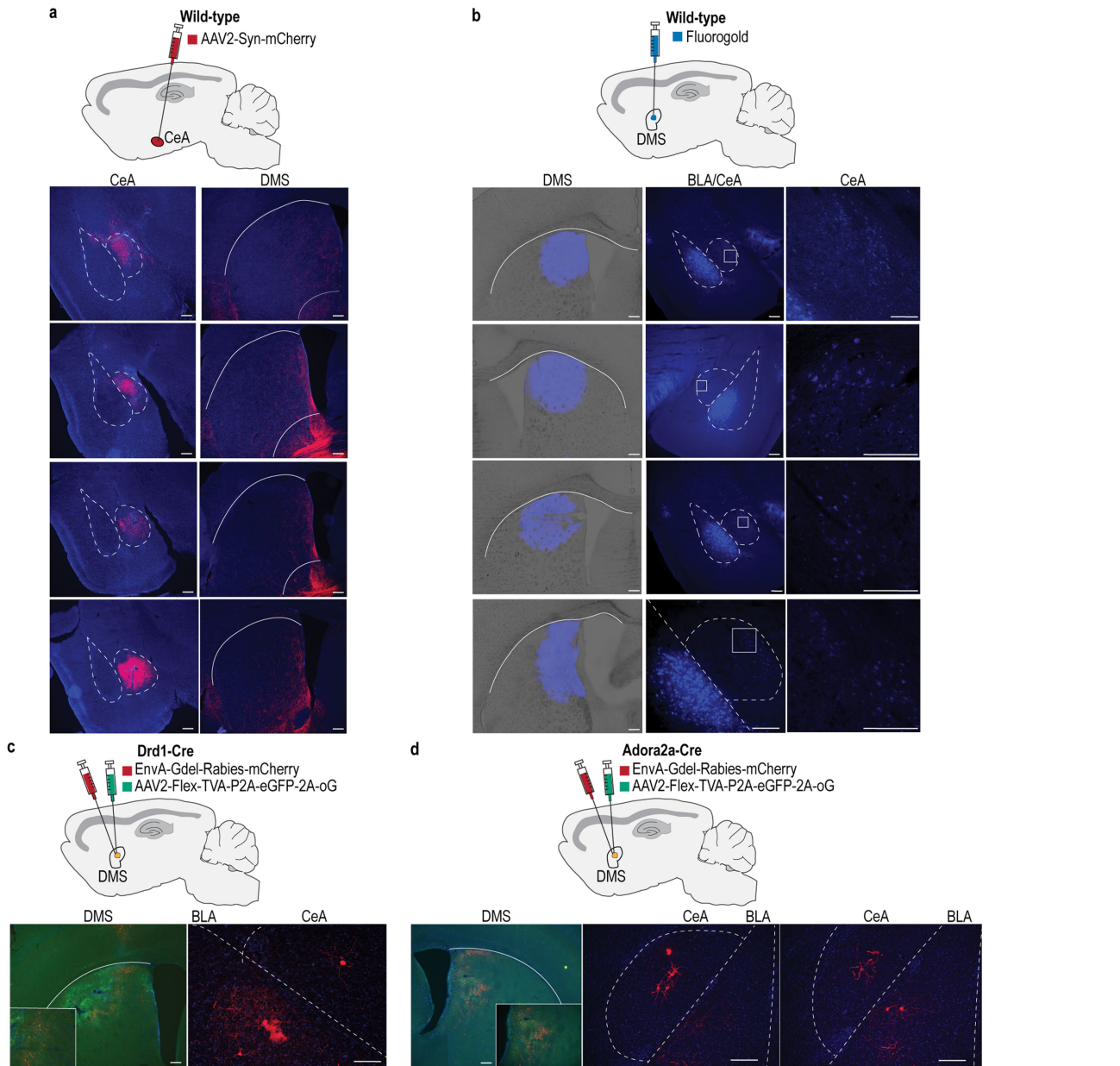


Extended Data Fig. 2 | Food-port entries during training and probe tests following handling control or chronic stress. (a) Food-port entry rate across training for subjects in the devaluation experiment. 2-way ANOVA: Training: $F_{(2,42,108,90)} = 3.17, P = 0.04$; Stress: $F_{(1,45)} = 0.07, P = 0.79$; Training x Stress: $F_{(3,135)} = 0.57, P = 0.64$. (b) Food-port entries during the devaluation probe tests. 2-way ANOVA: Value: $F_{(1,45)} = 6.77, P = 0.01$, Stress: $F_{(1,45)} = 0.29, P = 0.60$; Stress x Value: $F_{(1,45)} = 2.42, P = 0.13$. Control N = 22 (13 male), Stress N = 25 (12 male) mice. (c) Food-port entry rate across training for subjects in the contingency degradation experiment. 3-way ANOVA: Training: $F_{(2,84,62,10)} = 6.44, P = 0.001$; Stress: $F_{(1,25)} = 0.01, P = 0.91$; Future Contingency Degradation group: $F_{(1,25)} = 1.27, P = 0.27$; Training x Stress: $F_{(3,75)} = 1.62, P = 0.19$; Training x Group: $F_{(3,75)} = 0.24, P = 0.87$; Stress x Group: $F_{(1,25)} = 0.004, P = 0.95$; Training x Stress x Group: $F_{(3,75)} = 1.49, P = 0.23$. (d) Food-port entries during the probe test 24 h following contingency degradation or non-degraded control. 2-way ANOVA: Stress x Contingency Degradation Group: $F_{(1,25)} = 18.88, P = 0.0002$; Contingency Degradation: $F_{(1,25)} = 4.29, P = 0.05$; Stress: $F_{(1,25)} = 1.41, P = 0.25$. Control, Non-degraded N = 7 (3 male), Control, Degraded N = 7 (3 male), Stress Non-degraded N = 7 (3 male) Stress Degraded N = 8 (4 male) mice. Males = solid lines, Females = dashed lines. Data presented as mean +/- SEM. * $P < 0.05$, ** $P < 0.01$, corrected for multiple comparisons.



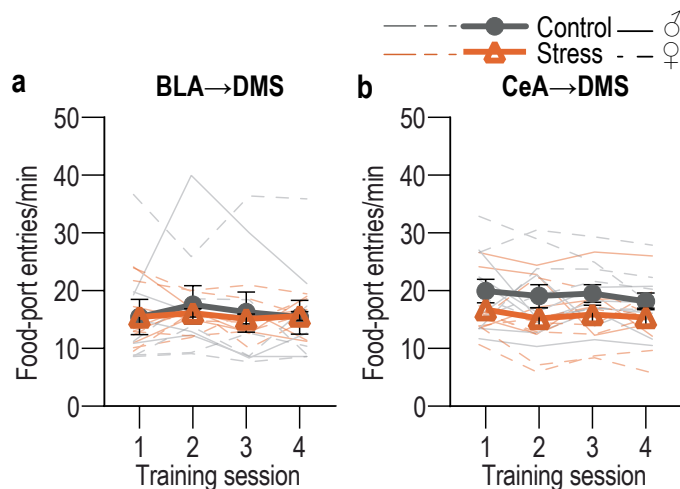
Extended Data Fig. 3 | Lever presses and food-port entries during contingency degradation. (a) Contingency degradation Procedure. Following stress and training, half the subjects in each group received a 20-min contingency degradation session during which lever pressing continued to earn reward with a probability of 0.1, but reward was also delivered non-contingently with the same probability. This session was identical for non-degraded controls, except they did not receive free rewards. (b) 3-way ANOVA: Press rate in 1-min bins during the contingency degradation session. Time x Contingency Degradation Group: $F_{(19,475)} = 2.03, P = 0.0063$; Time x Stress: $F_{(19,475)} = 2.43, P = 0.0007$; Stress x Group: $F_{(1,25)} = 0.0001, P = 0.99$; Time: $F_{(9,17,229,20)} = 2.13, P = 0.03$; Stress: $F_{(1,25)} = 1.36, P = 0.26$; Degradation Group: $F_{(1,25)} = 68.23, P < 0.0001$; Time x Stress x Degradation Group: $F_{(19,475)} = 1.30, P = 0.19$. Contingency degradation cause lower press rates across the session in both control (Time x Contingency Degradation Group: $F_{(12,228)} = 2.47, P = 0.0009$; Time: $F_{(6,62,79,39)} = 2.47, P = 0.03$;

Degradation Group: $F_{(1,12)} = 45.16, P < 0.0001$) and stressed (Contingency Degradation Group: $F_{(1,13)} = 28.22, P = 0.0001$; Time: $F_{(6,01,78,16)} = 2.19, P = 0.05$; Time x Contingency Degradation Group: $F_{(19,247)} = 1.10, P = 0.35$) mice. (c) Rate of entry into the food-delivery port in 1-min bins during the contingency degradation session. 3-way ANOVA: Time x Contingency Degradation Group: $F_{(19,475)} = 3.80, P < 0.0001$; Time x Stress: $F_{(19,475)} = 1.20, P = 0.26$; Stress x Group: $F_{(1,25)} = 0.006, P = 0.94$; Time: $F_{(6,26,156,60)} = 7.53, P < 0.0001$; Stress: $F_{(1,25)} = 2.51, P = 0.13$; Degradation Group: $F_{(1,25)} = 1.37, P = 0.5$; Time x Stress x Degradation Group: $F_{(19,475)} = 0.86, P = 0.63$. Control, Non-degraded N = 7 (3 male), Control, Degraded N = 7 (3 male), Stress Non-degraded N = 7 (3 male) Stress Degraded N = 8 (4 male) mice. Males = closed circles/solid lines, Females = open circles/dashed lines. Data presented as mean +/- SEM. * $P < 0.05$, ** $P < 0.01$, corrected for multiple comparisons.

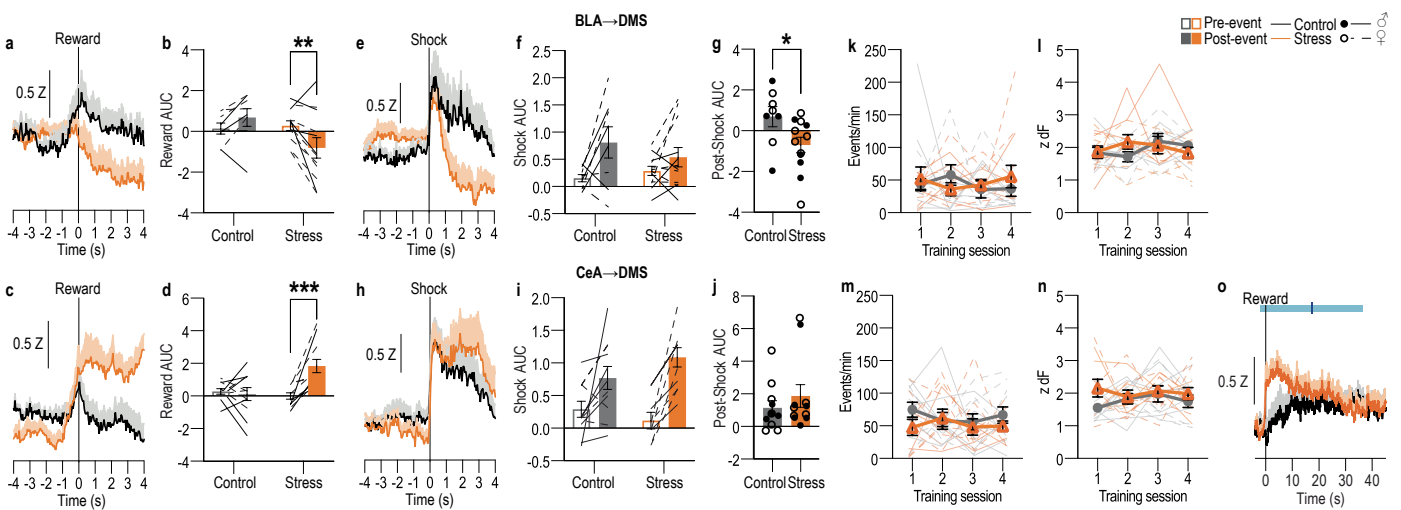


Extended Data Fig. 4 | BLA and CeA directly project to DMS. (a) Top: Anterograde tracing approach. Infusion of an AAV expressing mCherry into the CeA. Bottom: mCherry labeling at infusion site in CeA (left) and mCherry-labeled fibers in the DMS (right). N = 4 (2 male) mice. We observed mCherry-expressing putative fibers in the DMS but not dorsolateral striatum. Expression was also detected in other well-known CeA projection targets such as the bed nucleus of the stria terminalis. (b) Top: Retrograde tracing approach. We infused the fluorescently labeled retrograde tracer Fluorogold into the DMS. Bottom: Fluorogold labeling at infusion site in DMS (left) and fluorogold-labeled, DMS-projecting cell bodies in BLA and CeA (middle), with CeA magnified (right). Labeled cells were detected in both BLA and CeA, indicating that both BLA and CeA directly project to DMS. Labeling was greater in BLA than CeA, indicating the BLA→DMS pathway is denser than the CeA→DMS pathway. N = 4 (2 male) mice. (c) Top: Approach for rabies trans-synaptic retrograde tracing of DMS Drd1⁺ striatal neurons. We used rabies tracing to confirm monosynaptic amygdala projections onto DMS neurons. We infused a

starter virus expressing cre-dependent TVA-oG-GFP into the DMS of mice expressing cre-recombinase under the control of dopamine receptor 1 (D1-Cre) or adenosine 2a receptor (A2a-Cre) genes^{101,102}, followed by ΔG-deleted rabies-mCherry to retrogradely label cells that synapse onto DMS D1 or A2a neurons. Bottom: Starter oG virus (green) and ΔG-deleted rabies-mCherry (red) expression in DMS Drd1⁺ neurons (left) and rabies-labeled, DMS DI-projecting cell bodies in the BLA and CeA (right), consistent with prior reports^{30,34}. Representative example from N = 4 (3 males) mice. (d) Top: Approach for rabies trans-synaptic retrograde tracing of DMS Adora2a⁺ neurons. Bottom: Starter ΔG virus (green) and rabies-mCherry (red) expression in DMS Adora2a⁺ neurons (left) and rabies-labeled, DMS A2A-projecting cell bodies in the BLA and CeA (right). Representative example N = 4 (3 males) mice. Scale bars = 200 μm. Combined, these data confirm that both BLA and CeA directly project to the DMS and are, thus, poised to influence the learning that supports goal-directed decision making and habit formation.



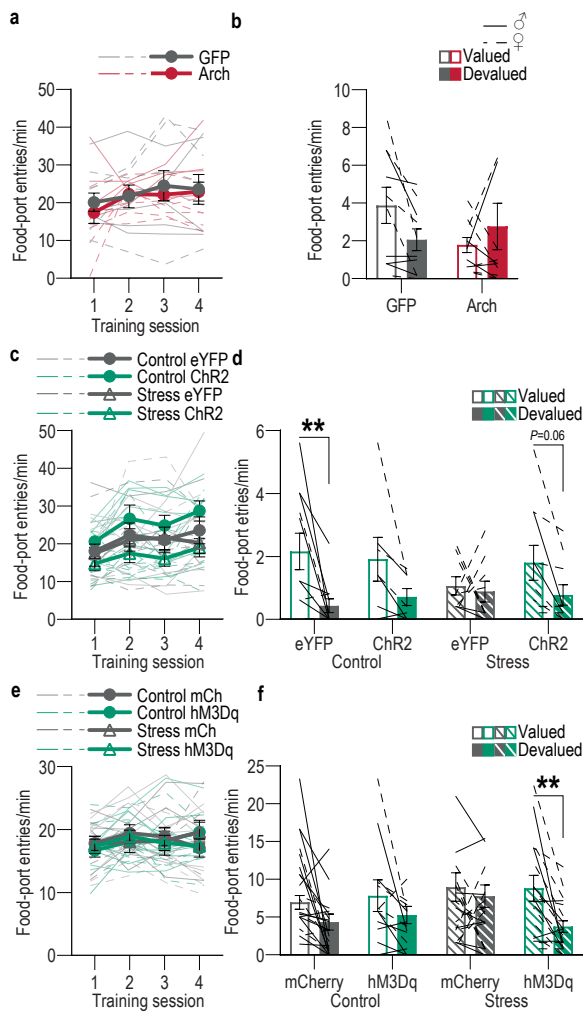
Extended Data Fig. 5 | Food-port entries during training with fiber photometry recording of BLA→DMS or CeA→DMS calcium activity following handling control or chronic stress. (a) Food-port entry rates across training for BLA→DMS GCaMP8s mice. 2-way ANOVA: Training: $F_{(2,47,46,99)} = 0.65, P = 0.56$; Stress: $F_{(1,19)} = 0.05, P = 0.82$; Training x Stress: $F_{(3,57)} = 0.24, P = 0.87$. BLA Control N = 9 (4 male), BLA Stress N = 12 (5 male) mice. (b) Food-port entry rates across training for CeA→DMS GCaMP8s mice. 2-way ANOVA: Training: $F_{(2,36,47,19)} = 0.89, P = 0.43$; Stress: $F_{(1,20)} = 2.71, P = 0.12$; Training x Stress: $F_{(3,60)} = 0.09, P = 0.96$. CeA Control N = 11 (6 male), CeA Stress N = 11 (4 male) mice. Males = solid lines, Females = dashed lines. Data presented as mean \pm SEM.



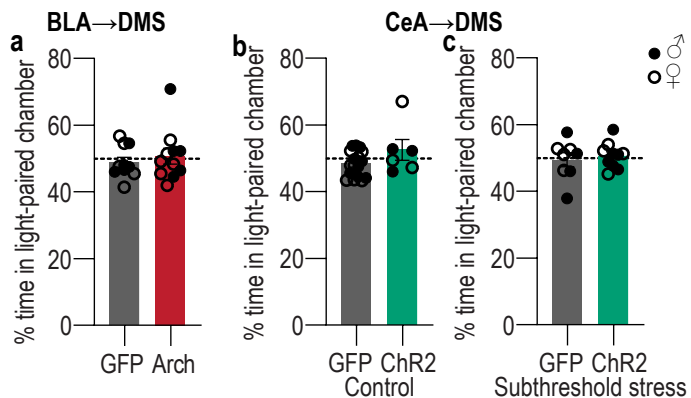
Extended Data Fig. 6 | BLA→DMS and CeA→DMS pathway baseline activity and pathway responses to unpredicted rewarding and aversive events in control and stressed mice. (a-j) Following instrumental training (Fig. 2), we used fiber photometry to record GCaMP8s fluorescent changes in either BLA (top) or CeA (bottom) neurons that project to the DMS in response to unpredicted food-pellet reward deliveries or unpredicted 2-s, 0.7 mA footshocks in control and stressed mice. (a) Trial-averaged Z-scored $\Delta f/F$ BLA→DMS GCaMP8s fluorescence changes around unpredicted food-pellet reward delivery. (b) Trial-averaged quantification of area under the BLA→DMS GCaMP8s Z-scored $\Delta f/F$ curve (AUC) during the 3-s period prior to (baseline) and following reward collection. 2-way ANOVA: Stress x Reward: $F_{(1,18)} = 10.88$, $P = 0.004$; Reward: $F_{(1,18)} = 1.19$, $P = 0.03$; Stress: $F_{(1,18)} = 1.77$, $P = 0.20$. (c) Trial-averaged Z-scored $\Delta f/F$ CeA→DMS GCaMP8s fluorescence changes around unpredicted food-pellet reward delivery. (d) Trial-averaged quantification CeA→DMS GCaMP8s Z-scored $\Delta f/F$ AUC during the 3-s period prior to and following reward collection. 2-way ANOVA: Stress x Reward: $F_{(1,20)} = 11.79$, $P = 0.02$; Reward: $F_{(1,20)} = 8.14$, $P = 0.01$; Stress $F_{(1,20)} = 4.49$, $P = 0.05$. (e) Trial-averaged Z-scored $\Delta f/F$ BLA→DMS GCaMP8s fluorescence changes around unpredicted footshock. (f) Trial-averaged quantification of BLA→DMS GCaMP8s Z-scored $\Delta f/F$ AUC during the 1-s acute shock response compared to a 1-s pre-shock baseline. 2-way ANOVA: Shock: $F_{(1,18)} = 8.53$, $P = 0.01$; Stress: $F_{(1,18)} = 0.14$, $P = 0.71$; Stress x Shock $F_{(1,18)} = 1.73$, $P = 0.21$. (g) Trial-averaged quantification of BLA→DMS GCaMP8s Z-scored $\Delta f/F$ AUC during 2-s post-shock period. 2-sided t-test: $t_{(18)} = 2.26$, $P = 0.04$, 95% CI -2.68 to -0.10. (h) Trial-averaged Z-scored $\Delta f/F$ CeA→DMS GCaMP8s fluorescence changes around unpredicted footshock. (i) Trial-averaged quantification of CeA→DMS GCaMP8s Z-scored $\Delta f/F$ AUC during the 1-s acute shock response, compared to baseline. 2-way ANOVA: Shock: $F_{(1,20)} = 28.24$, $P < 0.0001$; Stress: $F_{(1,20)} = 0.22$, $P = 0.64$; Stress x Shock: $F_{(1,20)} = 3.20$, $P = 0.09$. (j) Trial-averaged quantification of CeA→DMS GCaMP8s Z-scored $\Delta f/F$ AUC during 2-s post-shock period. 2-sided t-test: $t_{(20)} = 0.88$, $P = 0.39$, 95% CI -0.99 to -2.43. BLA Control N = 8 (4 male), BLA Stress N = 12 (5 male) mice. CeA Control N = 11 (6 male), CeA Stress N = 11 (4 male) mice. BLA→DMS projections are activated by unpredicted rewards and this is attenuated by prior chronic stress. Conversely, CeA→DMS projections are not

normally robustly activated by unpredicted rewards, but are activated by unpredicted rewards following chronic stress. Interestingly, unpredicted rewards robustly activated CeA→DMS projections here, but rewards did not evoke such a response early in instrumental training (Fig. 2m). Rather rewards responses developed with training. This indicates that stress-induced engagement of the CeA→DMS pathway may require repeated reward experience, which may reflect engagement of this pathway with repeated reinforcement and/or opportunity to learn the value or salience of the reward. We speculate this CeA→DMS engagement could be a compensatory mechanism triggered in response to the lack of engagement of the BLA→DMS pathway. Both BLA→DMS and CeA→DMS pathways are acutely activated by unpredicted footshock regardless of prior stress. Chronic stress reduces post-shock activity in the BLA→DMS pathway. (k-l) Frequency (k; 2-way ANOVA: Training: $F_{(2,41,45,69)} = 0.17$, $P = 0.88$; Stress: $F_{(1,19)} = 0.08$, $P = 0.78$; Training x Stress: $F_{(3,57)} = 0.85$, $P = 0.47$) and amplitude (l; 2-way ANOVA: Training: $F_{(2,48,47,10)} = 0.86$, $P = 0.45$; Stress: $F_{(1,19)} = 0.03$, $P = 0.85$; Training x Stress: $F_{(3,57)} = 1.37$, $P = 0.26$) of Z-scored $\Delta f/F$ spontaneous calcium activity of BLA→DMS projections during the 3-min baseline period prior to each training session in handled control and stressed mice. (m-n) Frequency (m; 2-way ANOVA: Training: $F_{(2,70,53,97)} = 0.21$, $P = 0.88$; Stress $F_{(1,20)} = 3.03$, $P = 0.10$; Training x Stress: $F_{(3,60)} = 0.55$, $P = 0.65$) and amplitude (n; 2-way ANOVA: Training: $F_{(2,59,51,83)} = 0.32$, $P = 0.78$; Stress: $F_{(1,20)} = 3.70$, $P = 0.07$; Training x Stress: $F_{(3,60)} = 0.75$, $P = 0.52$) of Z-scored $\Delta f/F$ spontaneous calcium activity of CeA→DMS projections during the 3-min baseline period prior to each training session handled control and stressed mice. Chronic stress did not alter baseline spontaneous calcium activity in either pathway. (o) Trial-averaged Z-scored $\Delta f/F$ CeA→DMS GCaMP8s fluorescence changes aligned to reward collection during training, with 40-s post-collection window. Blue line is the average time of the next lever press (light blue bar = s.e.m.). In stressed mice, CeA→DMS neurons respond to earned reward and this activity takes ~30 s on average to come back to baseline. Control N = 11 (6 male), Stress N = 11 (4 male) mice. Males = solid lines, Females = dashed lines. Data presented as mean +/- SEM. ** $P < 0.01$, corrected for multiple comparisons.

Article

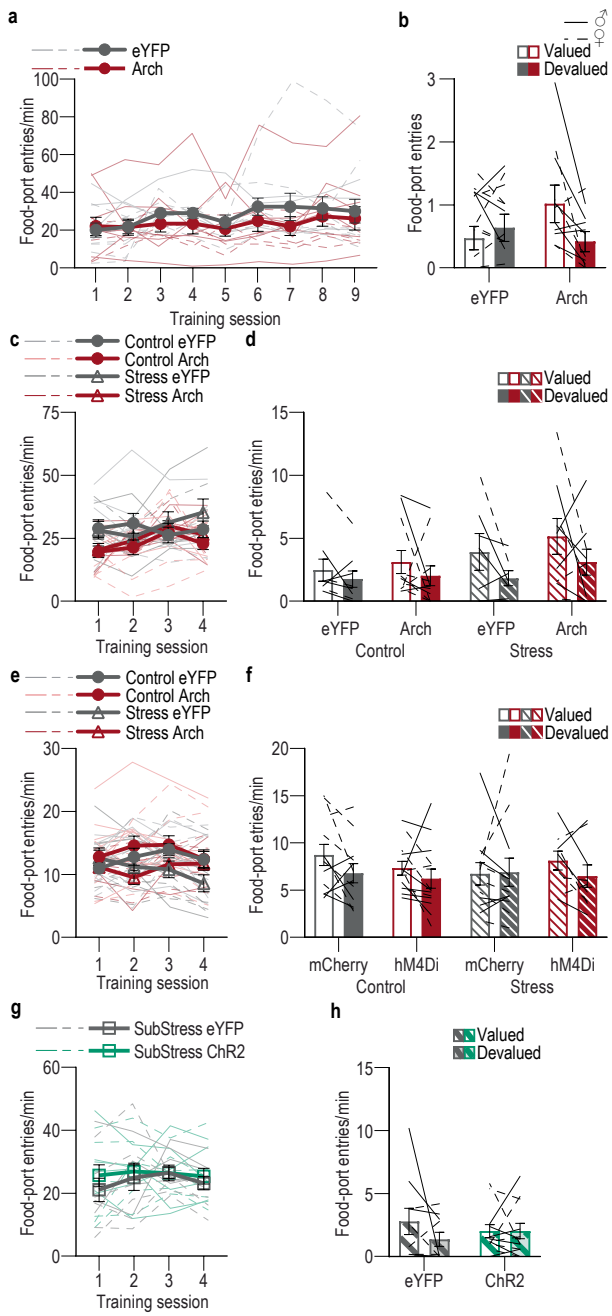


Extended Data Fig. 7 | Food-port entries during training with BLA→DMS manipulations and devaluation probe tests. **(a-b)** Optogenetic inactivation of BLA→DMS projections at reward during instrumental learning. **(a)** Food-port entries across training. 2-way ANOVA: Training: $F_{(2,03,38,55)} = 3.30, P = 0.05$; Virus: $F_{(1,19)} = 0.14, P = 0.71$; Training x Virus: $F_{(3,57)} = 0.43, P = 0.73$. **(b)** Food-port entry rates during devaluation probe tests. 2-way ANOVA: Stress x Value: $F_{(1,19)} = 4.38, P = 0.05$; Stress: $F_{(1,19)} = 0.47, P = 0.50$; Value: $F_{(1,19)} = 0.39, P = 0.54$. eYFP N = 10 (5 males), Arch N = 11 (5 male) mice. **(c-d)** Optogenetic activation of BLA→DMS projections during post-stress instrumental learning. **(c)** Food-port entry rate across training. 3-way ANOVA: Training: $F_{(2,5,82,82)} = 6.47, P = 0.001$; Stress: $F_{(1,33)} = 3.78, P = 0.06$; Virus: $F_{(1,33)} = 0.02, P = 0.89$; Training x Stress: $F_{(3,99)} = 0.67, P = 0.57$; Training x Virus: $F_{(3,99)} = 0.45, P = 0.72$; Stress x Virus: $F_{(1,33)} = 2.18, P = 0.15$; Training x Stress x Virus: $F_{(3,99)} = 0.26, P = 0.86$. **(d)** Food-port entry rate during the devaluation probe tests. 3-way ANOVA: Value: $F_{(1,33)} = 15.65, P = 0.0004$; Stress: $F_{(1,33)} = 0.23, P = 0.63$; Virus: $F_{(1,33)} = 0.20, P = 0.65$; Value x Stress: $F_{(1,33)} = 2.75, P = 0.11$; Value x Virus: $F_{(1,33)} = 0.09, P = 0.76$; Virus x Stress: $F_{(1,33)} = 0.17, P = 0.68$; Value x Stress x Virus: $F_{(1,33)} = 1.73, P = 0.20$. Control, Value: $F_{(1,16)} = 12.42, P = 0.003$; Virus: $F_{(1,16)} = 0.0007, P = 0.98$; Value x Virus: $F_{(1,16)} = 0.40, P = 0.53$. Stress, Value: $F_{(1,17)} = 3.46, P = 0.08$; Virus: $F_{(1,17)} = 0.45, P = 0.51$; Value x Virus: $F_{(1,17)} = 1.71, P = 0.21$. Control eYFP N = 11 (7 male), Control ChR2 N = 7 (4 males), Stress eYFP N = 9 (2 male), Stress ChR2 N = 10 Stress (3 male) mice. **(e-f)** Chemogenetic activation of BLA→DMS projections during post-stress instrumental learning. **(e)** Food-port entry rate across training. 3-way ANOVA: Training: $F_{(2,55,84,12)} = 1.64, P = 0.19$; Stress: $F_{(1,33)} = 0.05, P = 0.95$; Virus: $F_{(1,33)} = 0.08, P = 0.78$; Training x Stress: $F_{(3,99)} = 0.16, P = 0.92$; Training x Virus: $F_{(3,99)} = 0.21, P = 0.89$; Stress x Virus: $F_{(1,33)} = 0.02, P = 0.89$; Training x Stress x Virus: $F_{(3,99)} = 3.07, P = 0.03$. **(f)** Food-port entry rate during the devaluation probe test. Planned comparisons 2-sided t-test valued v. devalued, Control mCherry: $t_{(20)} = 1.88, P = 0.07, 95\% \text{ CI} -0.21 - 5.41$; Control hM3Dq: $t_{(10)} = 1.32, P = 0.20, 95\% \text{ CI} -1.40 - 6.54$; Stress mCherry: $t_{(16)} = 0.75, P = 0.46, 95\% \text{ CI} -2.04 - 4.44$; Stress hM3Dq: $t_{(18)} = 3.36, P = 0.002, 95\% \text{ CI} 2.01 - 8.16$. Control mCherry N = 12 (7 male), Stress mCherry N = 9 (5 male), Stress hM3Dq N = 10 Stress (5 male) mice. Males = solid lines, Females = dashed lines. Data presented as mean \pm SEM. ** $P < 0.01$, corrected for multiple comparisons.

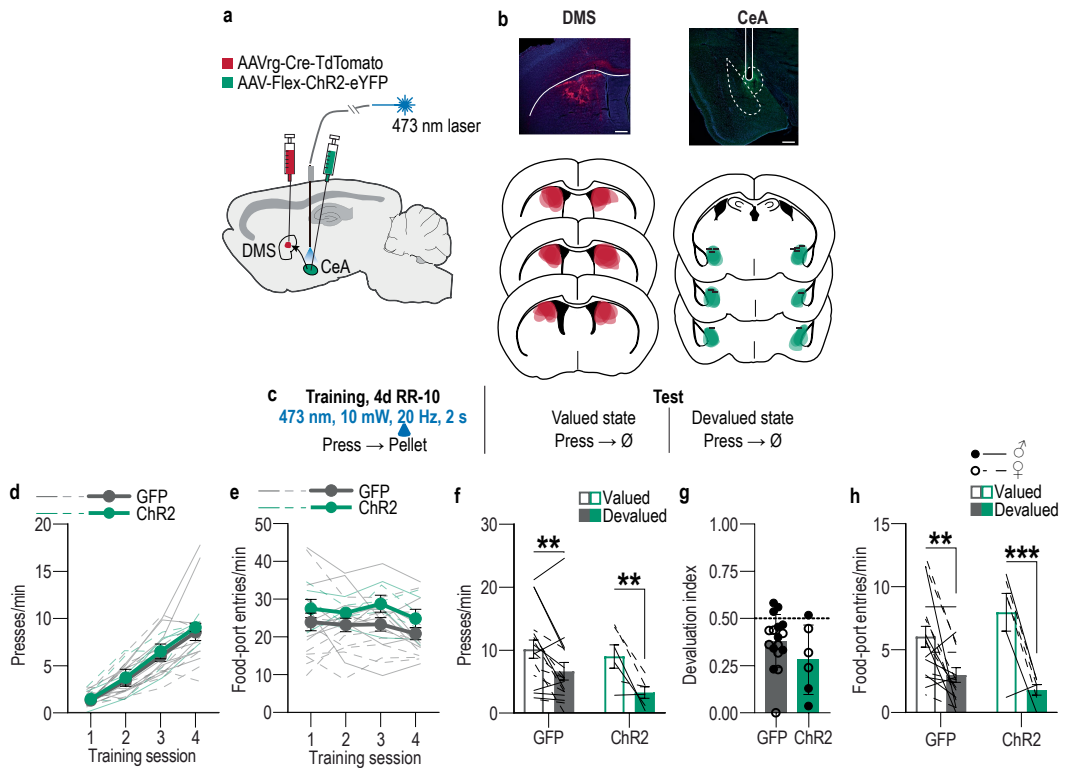


Extended Data Fig. 8 | Manipulation of BLA or CeA terminals in DMS is neither rewarding or aversive. (a) Following training and testing (Fig. 3h–n) mice receive a real-time place preference test in which 1 side of a 2-chamber apparatus was paired with optogenetic inhibition of BLA axons and terminals in the DMS. Average percent time spent in light-paired chamber across 2, 10-min sessions (one with light paired with each side). 2-sided t-test: $t_{(19)} = 0.65$, $P = 0.52$, 95% CI $-0.04 - 0.08$. eYFP N = 10 (5 male), Arch N = 11 (5 male) mice. Males = closed circles, Females = open circles. Data presented as mean \pm SEM. (b-c) Following training and testing mice receive a real-time place preference test in which 1 side of a 2-chamber apparatus was paired with optogenetic stimulation of DMS-projecting CeA neurons. (b) Average percent time spent in light paired chamber across 2, 10-min sessions (one with light paired with each side) in handled control subjects. 2-sided t-test: $t_{(21)} = 1.75$, $P = 0.10$, 95% CI $-0.79 - 9.06$. eYFP N = 17 (9 male), ChR2 N = 6 (3 male) mice. (c) Average percent time spent in light paired chamber across 2, 10-min sessions (one with light paired with each side) in subjects with a prior once/daily stress for 14 d. 2-sided t-test: $t_{(16)} = 0.52$, $P = 0.61$, 95% CI $-3.74 - 6.17$. eYFP N = 8 (4 male), ChR2 N = 10 (6 male) mice. Males = closed circles, Females = open circles. Data presented as mean \pm SEM.

Article



Extended Data Fig. 9 | Food-port entries during training with CeA→DMS manipulations and devaluation probe tests. **a–b** Optogenetic inhibition of CeA→DMS projections during instrumental overtraining. **(a)** Food-port entry rates across training. 2-way ANOVA: Training: $F_{(2,29,45,82)} = 1.81, P = 0.17$; Virus: $F_{(1,20)} = 0.67, P = 0.42$; Training x Virus: $F_{(8,160)} = 0.60, P = 0.77$. **(b)** Food-port entry rates during the devaluation probe tests. 2-way ANOVA: Virus x Value: $F_{(1,20)} = 4.51, P = 0.046$; Value: $F_{(1,20)} = 1.47, P = 0.24$; Virus: $F_{(1,20)} = 0.41, P = 0.53$; eYFP N = 11 (3 male), Arch N = 11 (7 male) mice. **(c–d)** Optogenetic inactivation of CeA→DMS projections at reward during post-stress learning. **(c)** Food-port entry rates across training. 3-way ANOVA: Training: $F_{(2,63,84,18)} = 3.21, P = 0.03$; Stress: $F_{(1,32)} = 0.60, P = 0.44$; Virus: $F_{(1,32)} = 4.75, P = 0.04$; Training x Stress: $F_{(3,96)} = 1.55, P = 0.21$; Training x Virus: $F_{(3,96)} = 2.42, P = 0.07$; Stress x Virus: $F_{(1,32)} = 0.04, P = 0.84$; Training x Stress x Virus: $F_{(3,96)} = 1.14, P = 0.34$. **(k)** Food-port entry rate during the devaluation probe test. 3-way ANOVA: Value x Stress x Virus: $F_{(1,32)} = 0.03, P = 0.86$; Value: $F_{(1,32)} = 6.44, P = 0.02$; Stress: $F_{(1,32)} = 2.02, P = 0.16$; Virus: $F_{(1,32)} = 1.09, P = 0.30$; Value x Stress: $F_{(1,3)} = 0.99, P = 0.33$; Value x Virus: $F_{(1,32)} = 0.02, P = 0.89$; Virus x Stress: $F_{(1,32)} = 0.24, P = 0.63$. **Control groups**, 2-way ANOVA: Value x Virus: $F_{(1,18)} = 0.09, P = 0.77$; Value: $F_{(1,18)} = 1.99, P = 0.17$; Virus: $F_{(1,18)} = 0.21, P = 0.65$. **Stress groups**, 2-way ANOVA: Value x Virus: $F_{(1,14)} = 0.0005, P = 0.98$; Value: $F_{(1,14)} = 3.94, P = 0.06$; Virus: $F_{(1,14)} = 0.85, P = 0.87$. Control eYFP N = 9 (5 male), Control Arch N = 11 (4 male), Stress eYFP N = 7 (6 male), Stress Arch N = 9 (5 male) mice. **(e–f)** Chemogenetic inhibition of CeA→DMS projections during post-stress instrumental learning. **(e)** Food-port entry rates across training. Training: $F_{(1,85,75,67)} = 2.02, P = 0.14$; Stress: $F_{(1,41)} = 4.42, P = 0.04$; Virus: $F_{(1,41)} = 0.41, P = 0.53$; Training x Stress: $F_{(3,123)} = 3.08, P = 0.03$; Training x Virus: $F_{(3,123)} = 0.64, P = 0.59$; Stress x Virus: $F_{(1,41)} = 0.20, P = 0.66$; Training x Stress x Virus: $F_{(3,123)} = 3.23, P = 0.02$. **(f)** Food-port entry rates during the devaluation probe tests. Planned comparisons 2-sided t-test valued v. devalued, Control mCherry: $t_{(11)} = 1.94, P = 0.06, 95\% \text{ CI} -0.25 - 12.07$; Control hM4Di: $t_{(12)} = 0.38, P = 0.71, 95\% \text{ CI} -4.81 - 7.03$; Stress mCherry: $t_{(10)} = 0.05, P = 0.96, 95\% \text{ CI} -6.33 - 5.99$; Stress hM4Di: $t_{(8)} = 0.47, P = 0.64, 95\% \text{ CI} -5.47 - 8.76$. Control mCherry N = 12 (5 male), Control hM4Di N = 13 (8 male), Stress mCherry N = 11 (5 male), Stress hM4Di N = 9 (4 male) mice. **(g–h)** Optogenetic stimulation of CeA→DMS projections at reward during learning following subthreshold once daily stress (SubStress). **(g)** Food-port entry rate across training. 2-way ANOVA: Training: $F_{(1,73,34,50)} = 0.89, P = 0.41$; Virus: $F_{(1,20)} = 0.46, P = 0.51$; Training x Virus: $F_{(3,60)} = 0.39, P = 0.76$. **(g)** Food-port entry rate during the devaluation probe test. 2-way ANOVA: Virus x Value: $F_{(1,20)} = 1.37, P = 0.26$; Virus: $F_{(1,20)} = 0.005, P = 0.94$; Value: $F_{(1,20)} = 1.36, P = 0.26$. eYFP N = 10 (4 male), ChR2 N = 12 (6 male) mice. Males = solid lines, Females = dashed lines. Data presented as mean \pm SEM.



Extended Data Fig. 10 | Optogenetic stimulation of CeA→DMS projections in control mice. (a) We used an intersectional approach to express the excitatory opsins Channelrhodopsin 2 (ChR2), or a fluorophore control in DMS-projecting CeA neurons and implanted optic fibers above the CeA. (b) Representative images of retro-cre expression in DMS and immunofluorescent staining of cre-dependent ChR2 expression in CeA (scale bars = 200 μ m) and map of retro-cre in DMS and cre-dependent ChR2 expression in CeA for all mice. (c) Procedure. Lever presses earned food pellet rewards on a random-ratio (RR) reinforcement schedule. We used blue light (473 nm, 10 mW, 20 Hz, 25-ms pulse width, 2 s) to stimulate CeA→DMS neurons during the collection of each earned reward in mice without a history of stress. Mice were then given a lever-pressing probe test in the Valued state, prefed on untrained food-pellet type to control for general satiety, and Devalued state prefed on trained food-pellet type to induce sensory-specific satiety devaluation (order counterbalanced). (d) Press rates across training. 2-way ANOVA: Training: $F_{(1,85,38,75)} = 62.18, P < 0.0001$;

Virus: $F_{(1,21)} = 0.23, P = 0.64$; Training x Virus: $F_{(3,63)} = 0.05, P = 0.98$. (e) Food-port entries across training. 2-way ANOVA: Training: $F_{(2,42,50,77)} = 2.00, P = 0.14$; Virus: $F_{(1,21)} = 1.85, P = 0.19$; Training x Virus: $F_{(3,63)} = 0.22, P = 0.88$. (f) Press rate during the devaluation probe test. 2-way ANOVA: Value: $F_{(1,21)} = 20.32, P = 0.0002$; Virus: $F_{(1,21)} = 0.92, P = 0.35$; Virus x Value: $F_{(1,21)} = 1.17, P = 0.29$. (g) Devaluation index. 2-sided t-test: $t_{(21)} = 1.37, P = 0.19$, 95% CI -0.25 - 0.05. (h) Food-port entries during the devaluation probe tests. 2-way ANOVA: Value: $F_{(1,21)} = 30.07, P < 0.0001$; Virus: $F_{(1,21)} = 0.12, P = 0.73$; Virus x Value: $F_{(1,21)} = 3.45, P = 0.08$. eYFP N = 17 (9 male), ChR2 N = 6 (3 male) mice. Data presented as mean \pm SEM. ** $P < 0.01$, *** $P < 0.001$, corrected for multiple comparisons. Optogenetic activation of CeA→DMS projections at reward during learning neither affects affect acquisition of the lever-press behavior, nor the action-outcome learning needed to support flexible goal-directed decision making during the devaluation test.

Reporting Summary

Nature Portfolio wishes to improve the reproducibility of the work that we publish. This form provides structure for consistency and transparency in reporting. For further information on Nature Portfolio policies, see our [Editorial Policies](#) and the [Editorial Policy Checklist](#).

Statistics

For all statistical analyses, confirm that the following items are present in the figure legend, table legend, main text, or Methods section.

n/a Confirmed

- The exact sample size (n) for each experimental group/condition, given as a discrete number and unit of measurement
- A statement on whether measurements were taken from distinct samples or whether the same sample was measured repeatedly
- The statistical test(s) used AND whether they are one- or two-sided
Only common tests should be described solely by name; describe more complex techniques in the Methods section.
- A description of all covariates tested
- A description of any assumptions or corrections, such as tests of normality and adjustment for multiple comparisons
- A full description of the statistical parameters including central tendency (e.g. means) or other basic estimates (e.g. regression coefficient) AND variation (e.g. standard deviation) or associated estimates of uncertainty (e.g. confidence intervals)
- For null hypothesis testing, the test statistic (e.g. F , t , r) with confidence intervals, effect sizes, degrees of freedom and P value noted
Give P values as exact values whenever suitable.
- For Bayesian analysis, information on the choice of priors and Markov chain Monte Carlo settings
- For hierarchical and complex designs, identification of the appropriate level for tests and full reporting of outcomes
- Estimates of effect sizes (e.g. Cohen's d , Pearson's r), indicating how they were calculated

Our web collection on [statistics for biologists](#) contains articles on many of the points above.

Software and code

Policy information about [availability of computer code](#)

Data collection

A detailed description of all data acquisition software is included in the manuscript methods. MedAssociates MedPC software versions IV and V were used to collect all operant behavioral data (instrumental training and testing; progressive ratio test). A custom workflow created in Bonsai version 2.4 was used to collect fiber photometry fluorescent emissions and simultaneously record timestamps of behavioral events. Biobserve software was used to conduct RTPP experiments. Anymaze software version 7.3 was used to collect behavioral data for open field test, elevated plus maze test, and light dark test. BZ-X Analyze software and Zeiss ZEN (blue edition) image acquisition software with used for imaging processing.

Data analysis

A detailed description of all data analysis procedures is included in the manuscript methods. Custom Matlab R2022b scripts were written to process and analyze fiber photometry data. Custom Matlab code for fiber photometry analysis written for a previous study and modified for this study is available online (<https://doi.org/10.5281/zenodo.4926719>). FIJI was used for image processing. GraphPad Prism Versions 9-11, Microsoft Excel, and SPSS were used for data processing and statistical analyses.

For manuscripts utilizing custom algorithms or software that are central to the research but not yet described in published literature, software must be made available to editors and reviewers. We strongly encourage code deposition in a community repository (e.g. GitHub). See the Nature Portfolio [guidelines for submitting code & software](#) for further information.

Data

Policy information about [availability of data](#)

All manuscripts must include a [data availability statement](#). This statement should provide the following information, where applicable:

- Accession codes, unique identifiers, or web links for publicly available datasets
- A description of any restrictions on data availability
- For clinical datasets or third party data, please ensure that the statement adheres to our [policy](#)

Data and code availability

All data that support the findings of this study are available in the source data accompanying this paper and from the corresponding author upon request. Custom-written MATLAB code is accessible via Dryad repository¹ and available from the corresponding author upon request.

¹ Wassum, K. et al. (Dryad, 2021).

Human research participants

Policy information about [studies involving human research participants](#) and [Sex and Gender in Research](#).

Reporting on sex and gender	<input type="button" value="not applicable"/>
Population characteristics	<input type="button" value="not applicable"/>
Recruitment	<input type="button" value="not applicable"/>
Ethics oversight	<input type="button" value="not applicable"/>

Note that full information on the approval of the study protocol must also be provided in the manuscript.

Field-specific reporting

Please select the one below that is the best fit for your research. If you are not sure, read the appropriate sections before making your selection.

Life sciences Behavioural & social sciences Ecological, evolutionary & environmental sciences

For a reference copy of the document with all sections, see nature.com/documents/nr-reporting-summary-flat.pdf

Life sciences study design

All studies must disclose on these points even when the disclosure is negative.

Sample size	Number of animals per group was informed by power analyses performed on previously-collected data to generate group sizes that ensured minimally sufficient statistical power (0.9) to detect statistically significant differences between groups (0.05), using mixed ANOVA and appropriate post-hoc tests adjusted for multiple comparisons. Sample size included expected attribution due to misplaced fibers and virus and to ensure counterbalancing of sex, viral group (if applicable), stress group (if application), outcome type, and test order.
Data exclusions	Exact number of excluded subjects for each experiment are included in the manuscript methods. Subjects were excluded for viral or optical fiber mistargeting or failure to complete instrumental training in the required number of sessions. For fiber photometry experiments, subjects were also excluded from one cohort based on missing recordings for one training session.
Replication	Each experiment was replicated at least twice, and all groups were represented in all cohorts. All attempts at replication were successful.
Randomization	Animals were randomly assigned to stress, virus, outcome type, and test order groups.
Blinding	Experimenters were not blinded to subject group during stress exposure, training, or testing as they administered viral infusions during surgery and stress exposures, but data was collected automatically using computer software. Experimenters were blinded to subject group during histology processing and determination of exclusions based on mistargeting.

Reporting for specific materials, systems and methods

We require information from authors about some types of materials, experimental systems and methods used in many studies. Here, indicate whether each material, system or method listed is relevant to your study. If you are not sure if a list item applies to your research, read the appropriate section before selecting a response.

Materials & experimental systems

n/a	Involved in the study
<input type="checkbox"/>	<input checked="" type="checkbox"/> Antibodies
<input checked="" type="checkbox"/>	<input type="checkbox"/> Eukaryotic cell lines
<input checked="" type="checkbox"/>	<input type="checkbox"/> Palaeontology and archaeology
<input type="checkbox"/>	<input checked="" type="checkbox"/> Animals and other organisms
<input checked="" type="checkbox"/>	<input type="checkbox"/> Clinical data
<input checked="" type="checkbox"/>	<input type="checkbox"/> Dual use research of concern

Methods

n/a	Involved in the study
<input checked="" type="checkbox"/>	<input type="checkbox"/> ChIP-seq
<input checked="" type="checkbox"/>	<input type="checkbox"/> Flow cytometry
<input checked="" type="checkbox"/>	<input type="checkbox"/> MRI-based neuroimaging

Antibodies

Antibodies used

Specific antibodies, vendors, catalog numbers, and lot numbers used in this study are listed in manuscript Supplemental Table 5.

Validation

All antibodies used in this study were commercially developed and validated. Validation data, instructions for use, and references can be found on each manufacturer's website.

Chicken anti-GFP: <https://www.abcam.com/gfp-antibody-ab13970.html>
 Chicken anti-mCherry: <https://www.abcam.com/products/primary-antibodies/mcherry-antibody-ab205402.html>
 Rabbit anti-DsRed: <https://www.takarabio.com/products/antibodies-and-elisa/fluorescent-protein-antibodies/red-fluorescent-protein-antibodies>
 Goat anti-chicken Alexa 488: <https://thermofisher.com/antibody/product/Goat-anti-Chicken-IgY-H-L-Cross-Adsorbed-Secondary-Antibody-Polyclonal/A32931>
 Goat anti-rabbit Alexa 594: <https://thermofisher.com/antibody/product/Goat-anti-Rabbit-IgG-H-L-Cross-Adsorbed-Secondary-Antibody-Polyclonal/A-11012>

Animals and other research organisms

Policy information about [studies involving animals](#); [ARRIVE guidelines](#) recommended for reporting animal research, and [Sex and Gender in Research](#)

Laboratory animals

Number, age, strain, and sex of subjects is included for each experiment in the manuscript methods. C57/Bl6J mice aged 8-12 weeks purchased from Jackson Laboratories were used for tracing, behavioral, and fiber photometry experiments. Drd1-Cre and Adora2A-Cre transgenic mice were bred in house and used for rabies tracing experiments.

Wild animals

This study did not include the use of wild animals.

Reporting on sex

Male and female mice of approximately equal number were used for all experiments. Sex was included as a factor in ANOVA for behavioral results in Figure 1. No statistical effect of sex was found. Males and female data was pooled for subsequent experiments, but these experiments were not powered to detect sex differences. Male and female data points are visually disaggregated in all figures.

Field-collected samples

This study did not include field-collected samples.

Ethics oversight

All procedures were conducted in accordance with the NIH Guide for the Care and Use of Laboratory Animals and were approved by the UCLA Institutional Animal Care and Use Committee.

Note that full information on the approval of the study protocol must also be provided in the manuscript.